Lattice-Boltzmann Method (LBM) Applied for the Fluid Dynamic Characterisation of (porous or non-spherical) Agglomerates

1844 – 1906

M. Sommerfeld, M. Dietzel,
M. Ernst and Y. Cui

Mechanische Verfahrenstechnik
Zentrum für Ingenieurwissenschaften
Martin-Luther-Universität
Halle-Wittenberg
D-06099 Halle (Saale), Germany

www-mvt.iw.uni-halle.de

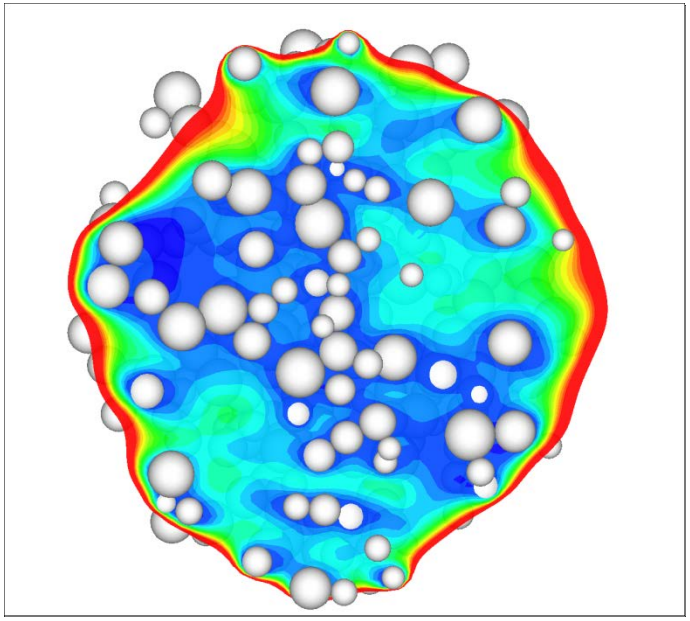

Content of the Lecture

- **Importance of agglomerates**
- **Fundamentals of the Lattice-Boltzmann Method (LBM)**
  - ★ curved wall boundary condition
  - ★ local grid refinement
  - ★ grid dependence, validation
- **Determination of fluid dynamic forces (drag force):**
  - ★ nearly spherical agglomerates
  - ★ nearly spherical fractal flocks
  - ★ carrier particle covered with small particles
- **Conclusions and Outlook**

Importance of Agglomerates

☞ **Agglomerates with complex structures and particle clusters are found in numerous technical and industrial applications.**

Agglomerate from spray drying

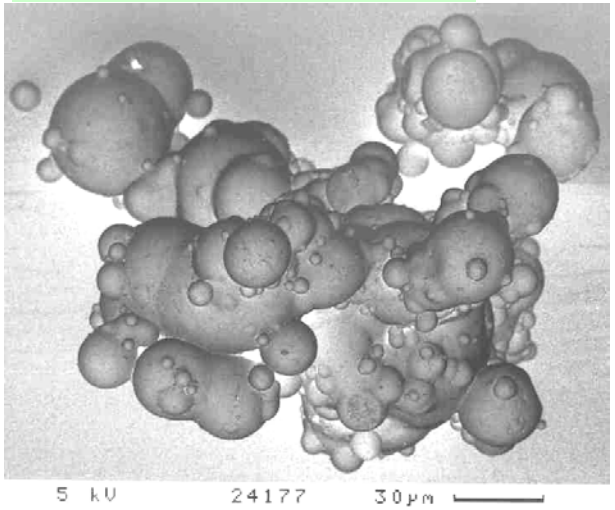

Agglomerate from flame synthesis

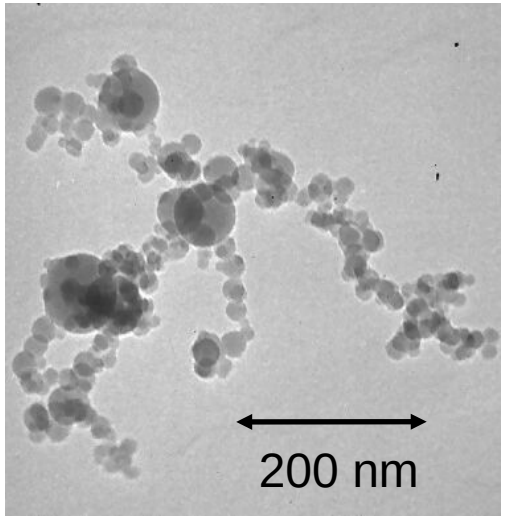

Formulation for medical applications

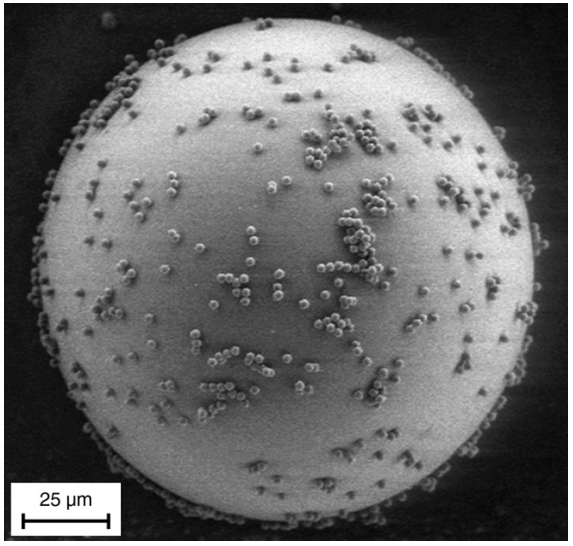

☞ **A numerical calculation of particle-laden flows with agglomerates and clusters cannot be properly done based on the volume equivalent diameter.**

☞ **Therefore DNS based on the Lattice-Boltzmann Method is performed for evaluating the fluid dynamic forces on agglomerates and particle clusters.**

Lattice-Boltzmann-Method (LBM) 1

- **Lattice-Boltzmann method is based on simulating the motion of discrete fluid elements in order to predict the macroscopic flow system.**
- **LBM is a very robust method for complex geometries.**
- **The variable of the Boltzmann statistics is the distribution function f($\underline{x}$, $\underline{v}$, t) which declares the number of fluid elements having the velocity $\underline{v}$ at the location $\underline{x}$ and time t.**
- **Macroscopic properties are related to the moments of the probability function:**

$$m = \int_{v^3}\int_{x^3} f\,(\underline{x}, \underline{v}, t)\, d^3x\, d^3v$$

$$\rho(\underline{x}, t) = \int_{v^3} f\, d^3v$$

$$\rho(\underline{x}, t)\,\underline{u}(\underline{x}, t) = \int_{v^3} \underline{v}\, f\, d^3v$$

discretisation

$$\rho(\mathbf{x}, t) = \sum_{\sigma}\sum_{i} f_{\sigma i}(\mathbf{x}, t)$$

$$\rho(\mathbf{x}, t)\,\mathbf{u}(\mathbf{x}, t) = \sum_{\sigma}\sum_{i} \underline{v}_{\sigma i}\, f_{\sigma i}(\mathbf{x}, t)$$

$$p(\mathbf{x}, t) = c_s^{\,2}\,\rho(\mathbf{x}, t) = \frac{1}{3}\frac{\Delta x^2}{\Delta t^2}\,\rho(\mathbf{x}, t)$$

$$\mu = \frac{1}{6}\rho c^2 (2\tau - \Delta t)$$

Lattice-Boltzmann-Methode 2

- **Boltzmann equation (rate of change of f($\underline{x}$, $\underline{v}$, t) due to transport and collision) with single relaxation approach (Bhatnagar Gross Krook (BGK) equation):**

$$\left(\frac{\partial}{\partial t} + \underline{v} \cdot \underline{\nabla}\right) f\left(\underline{x}, \underline{v}, t\right) = -\frac{1}{\tau}\left(f\left(\underline{x}, \underline{v}, t\right) - f^{(0)}\left(\underline{x}, \underline{v}, t\right)\right)$$

- **discretization in space, velocity and time:**
  - space is represented by a numerical **lattice**
  - predefined number of discrete velocity directions
  - propagation velocity: $c = \frac{\Delta x}{\Delta t} = \text{const} = \sqrt{3}\, c_s$
  - **Discrete velocities:**

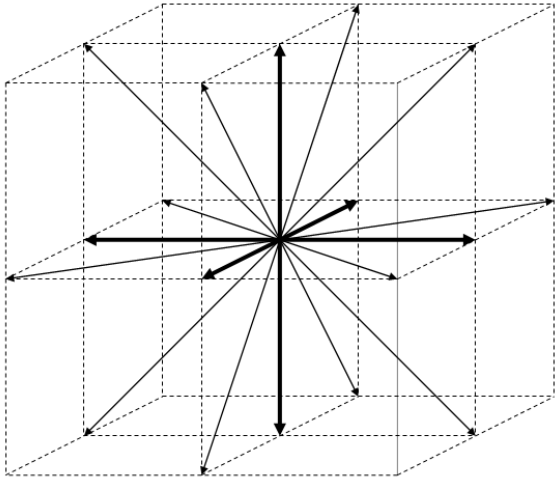

D3Q19-Model

$$\vec{\xi}_{\sigma i} = \begin{cases} (0,0,0), & \sigma = 0, \quad i = 1 \\ (\pm 1,0,0)c, (0,\pm 1,0)c, (0,0,\pm 1)c & \sigma = 1, \quad i = 1 \ldots 6 \\ (\pm 1,\pm 1,0)c, (\pm 1,0,\pm 1)c, (2,\pm 1,\pm 1)c, & \sigma = 2, \quad i = 1 \ldots 12 \end{cases}$$

$$\xi_{\sigma i} = \frac{\Delta x_{\sigma i}}{\Delta t}$$

τ: relaxation parameter, e.g. 0.515

Lattice-Boltzmann-Methode 3

- **Lattice Boltzmann equation und discretised equilibrium distribution:**

Propagation term **Collision term**

$$f_{\sigma i}\left(\mathbf{x}+\boldsymbol{\xi}_{\boldsymbol{\sigma}\mathbf{i}}\Delta t, t+\Delta t\right) - f_{\sigma i}\left(\mathbf{x},t\right) = -\frac{\Delta t}{\tau}\left(f_{\sigma i}\left(\mathbf{x},t\right) - f_{\sigma i}^{(0)}\left(\mathbf{x},t\right)\right) \qquad Ma = \frac{u}{c_s} << 1$$

$$f_{\sigma i}^{(0)}(\mathbf{x},t) = \omega_{\sigma i}\,\rho\left(1+\frac{3\boldsymbol{\xi}_{\boldsymbol{\sigma}\mathbf{i}}\,\mathbf{u}}{c^2}+\frac{9\left(\boldsymbol{\xi}_{\boldsymbol{\sigma}\mathbf{i}}\,\mathbf{u}\right)^2}{2c^4}-\frac{3\mathbf{u}^2}{2c^2}\right) \qquad \omega_{\sigma i} = \begin{cases} 1/3\,; & \sigma = 0,\ i = 1 \\ 1/18; & \sigma = 1,\ i = 1\ldots 6 \\ 1/36; & \sigma = 2,\ i = 1\ldots 12 \end{cases}$$

equilibrium distribution f_0: (Maxwellian distribution for Kn << 1)

$$f^{(0)}\left(\mathbf{x},\boldsymbol{\xi},t\right) = \frac{\rho}{\left(2\pi c_s^2\right)^{\frac{3}{2}}}\, e^{\frac{(\boldsymbol{\xi}-\mathbf{u})^2}{2c_s^2}}$$

- **Iteration cycle:**
  - Propagation
  - Relaxation (Collision)

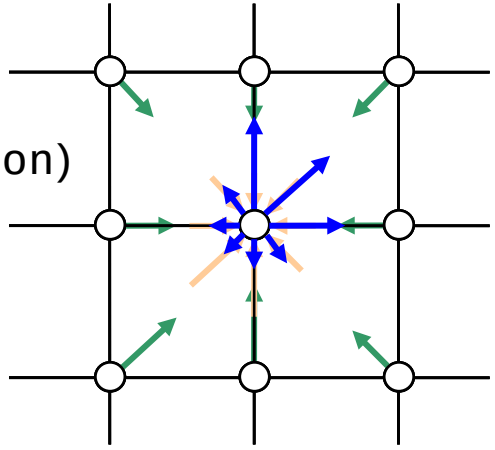

point of time: $t^* - \Delta t$

Martin-Luther-Universität Halle-Wittenberg

Lattice-Boltzmann-Methode 4

Standard wall boundary condition

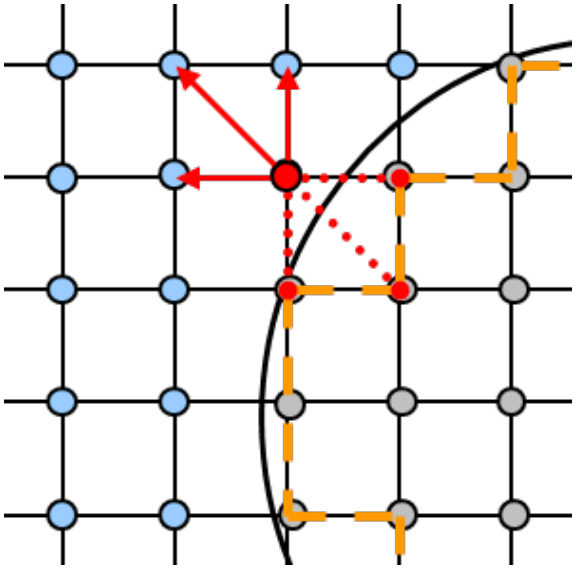

Extended wall boundary condition for curved walls Guo et al. (2002)

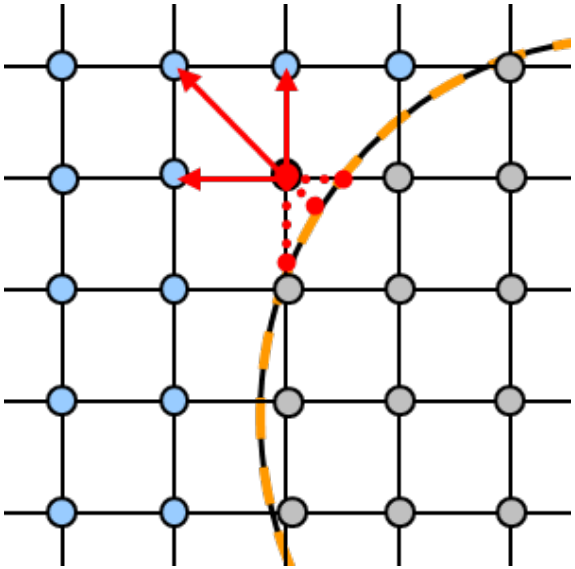

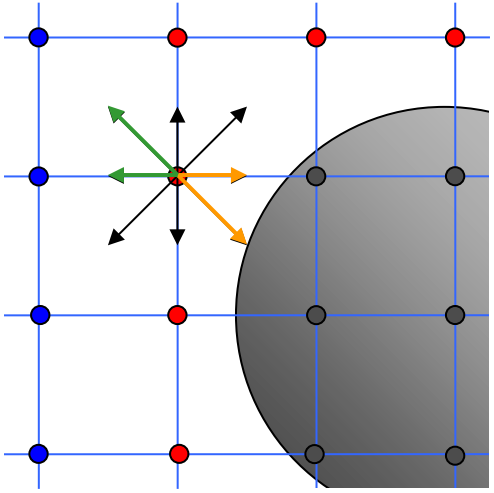

Forces over the surface of an object (particle) are obtained from a momentum balance (refection of the fluid elements)

$$\mathbf{F}_{\sigma\mathbf{i}}(\mathbf{x}, t+\Delta t/2) = \frac{\Delta V}{\Delta t}\left(f_{\sigma i}(\mathbf{x}, t+\Delta t) - f_{\sigma i}(\mathbf{x}, t^*)\right)\xi_{\sigma\mathbf{i}}$$

$$\mathbf{T}_{\sigma\mathbf{i}}(\mathbf{x}, t+\Delta t/2) = (\mathbf{x}-\mathbf{x}_{\mathbf{R}}) \times \mathbf{F}_{\sigma\mathbf{i}}(\mathbf{x}, t+\Delta t/2)$$

Lattice-Boltzmann-Methode 5

☞ Lattice-Boltzmann Method (LBM) with local grid refinement in order to increase locally spatial resolution:

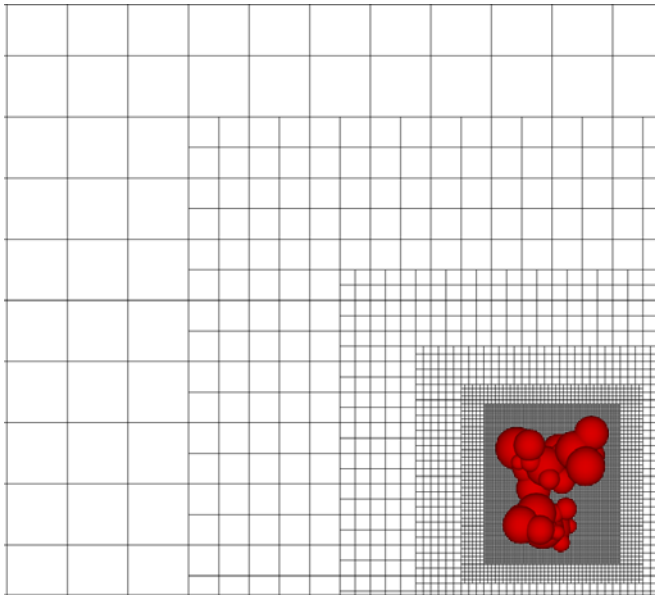

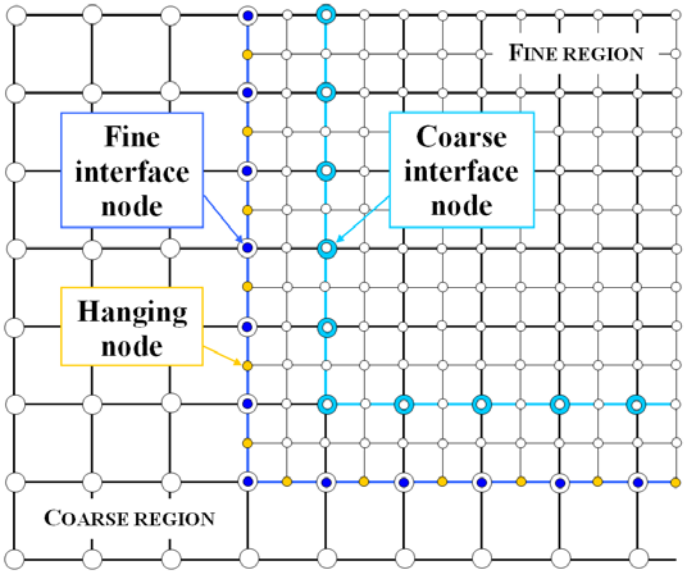

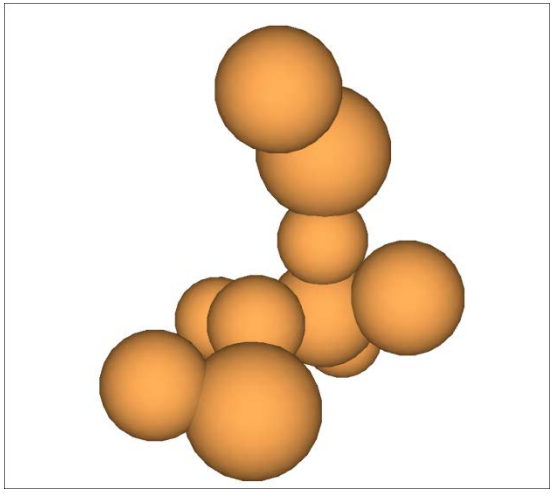

Real geometry

discretisation

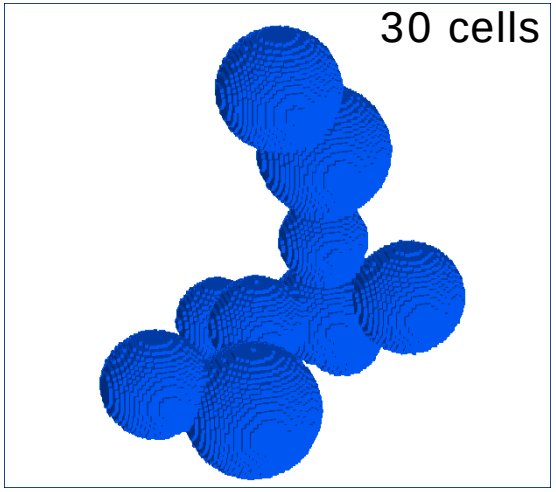

Resolved geometry

Definition of aerodynamic coefficients

- **Possible equivalent diameters:**

$$d_{equi} = \left\{ d_{VES}\,;\, r_{gyr}\,;\, d_{intercept}\,;\, d_{por}\,;\, d_{AES}\,;\, \ldots \right\}$$

- **Volume equivalent sphere:**

$$d_{VES} = \sqrt[3]{\frac{6}{\pi} V} \qquad A_{VES} = \sqrt[3]{\frac{9}{16} \pi V^2}$$

- **Drag coefficient:**

$$c_d = \frac{|\mathbf{F_d}|}{\frac{1}{2} \rho u^2 A_{equi}}$$

- **Lift coefficient:**

$$c_l = \frac{|\mathbf{F_l}|}{\frac{1}{2} \rho u^2 A_{equi}}$$

- **Torque coefficient:**

$$c_T = \frac{|\mathbf{T}|}{\frac{1}{2} \rho u^2 A_{equi}\, d_{equi}}$$

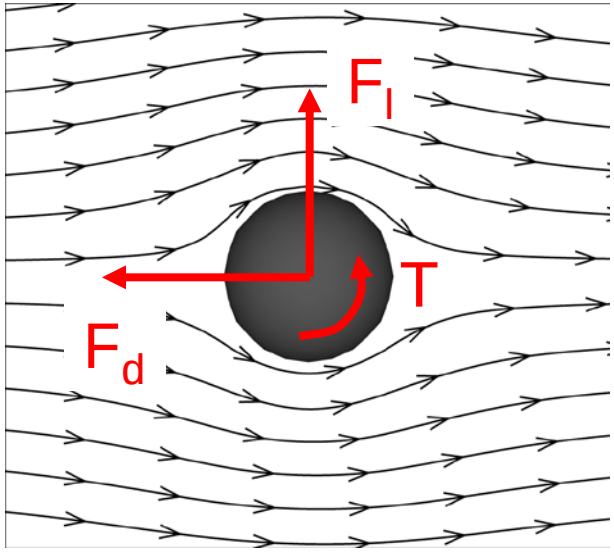

Grid Resolution Study

- ☞ **In the present studies the agglomerate or particle cluster is centrally fixed in a cubic computational domain and exposed to defined flow conditions**
- ☞ **The domain size and the resolution of the primary particles will affect the simulated fluid dynamic forces**

Computational domain and boundary conditions

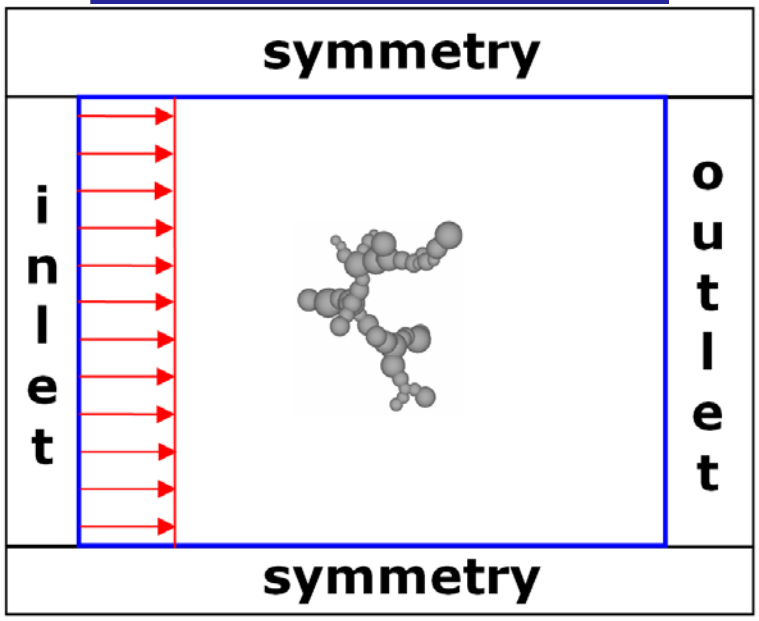

Domain size and spherical particle resolution without grid refinement

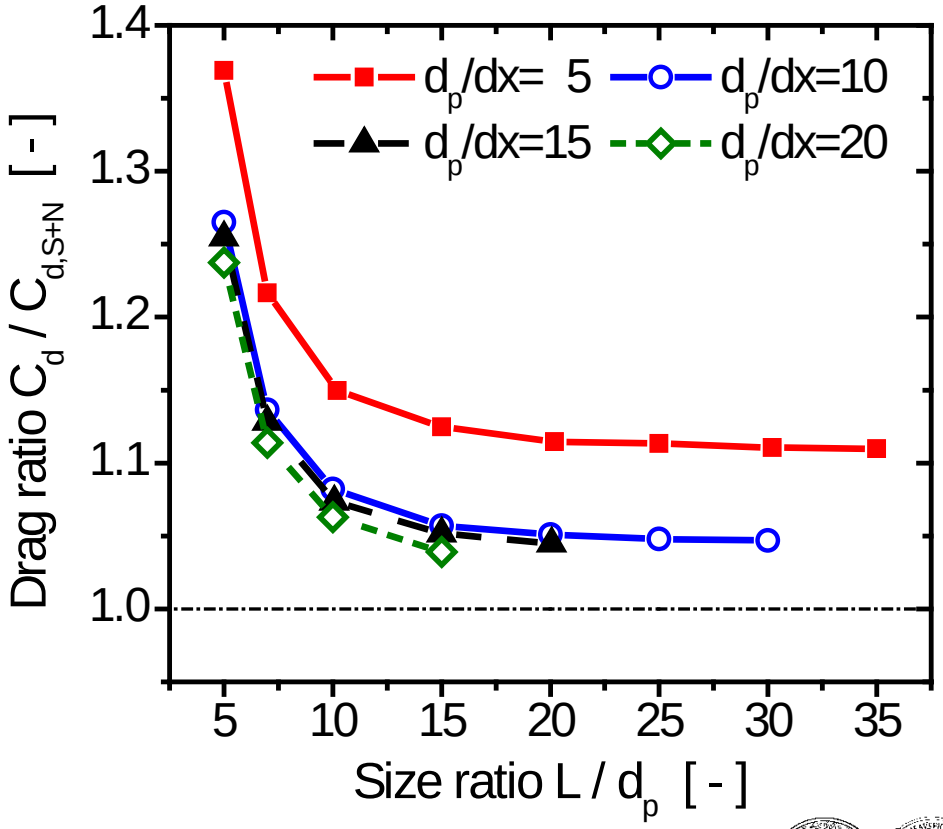

Validation of LBM Simulations

- **Verification of forces and coefficients by simulating the flow around spheres and cubes (laminar flow regime)**

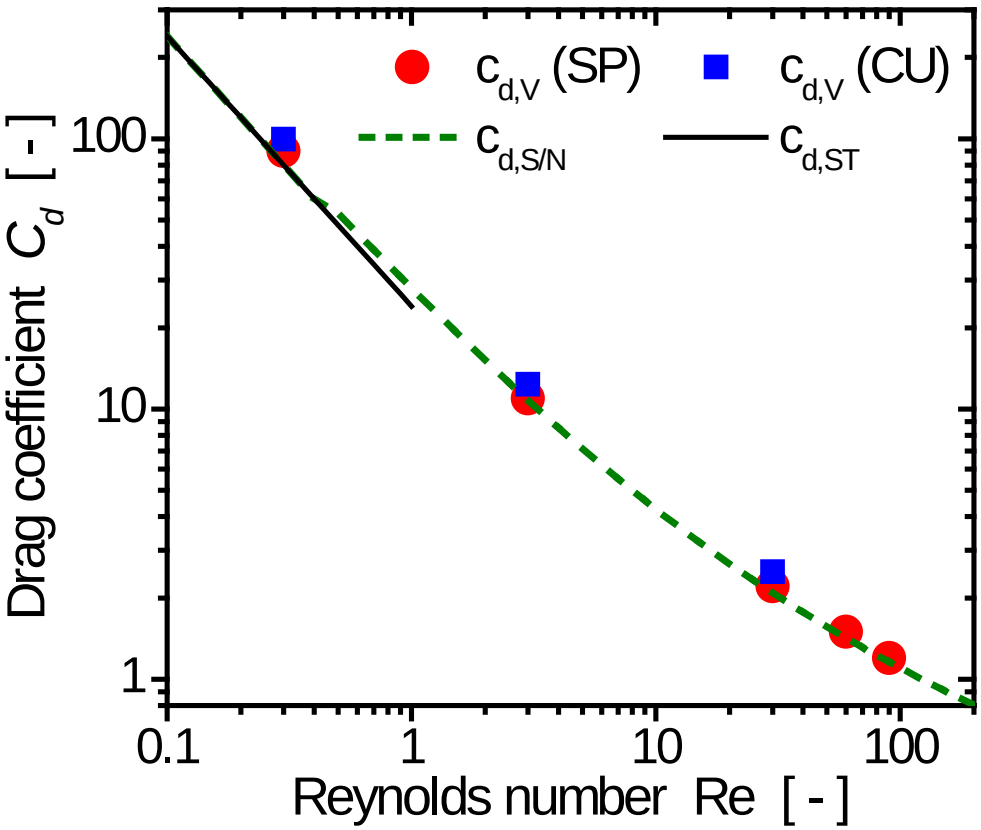

- Reynolds range: 0.3, 3, 30, 60, 90 (increase of D_P for higher Re)
- refinement levels: 5 ($\Delta x_c / \Delta x_f$ = 32/1)
- cells per diameter: 16 … 128
- Domain size: L/D_p = 50 up 400
- number of fluid nodes: max. 4.5 to 7.0 million

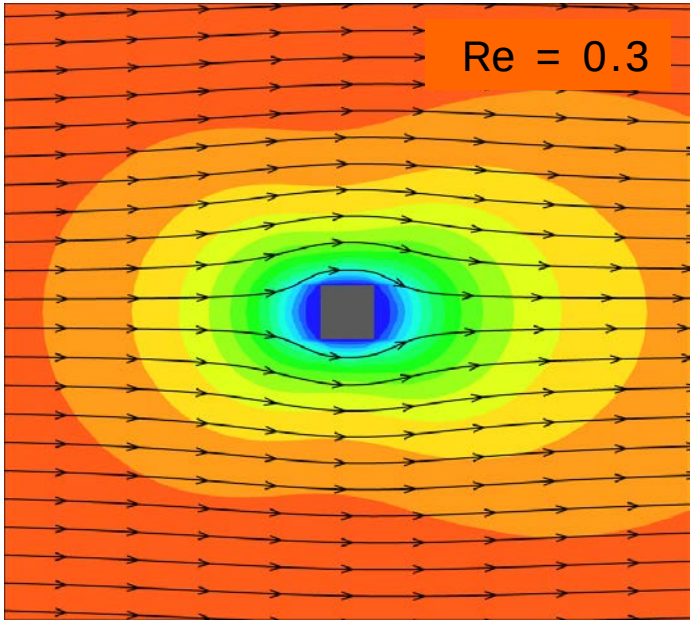

Validation: Particle Sitting on a Wall under Shear Flow

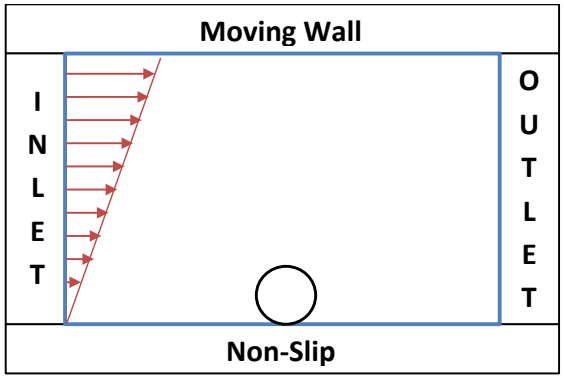

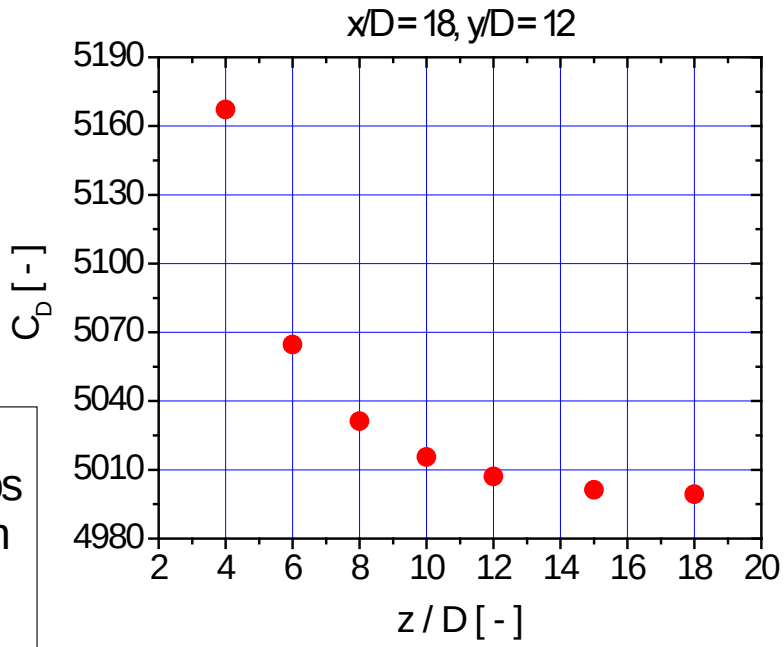

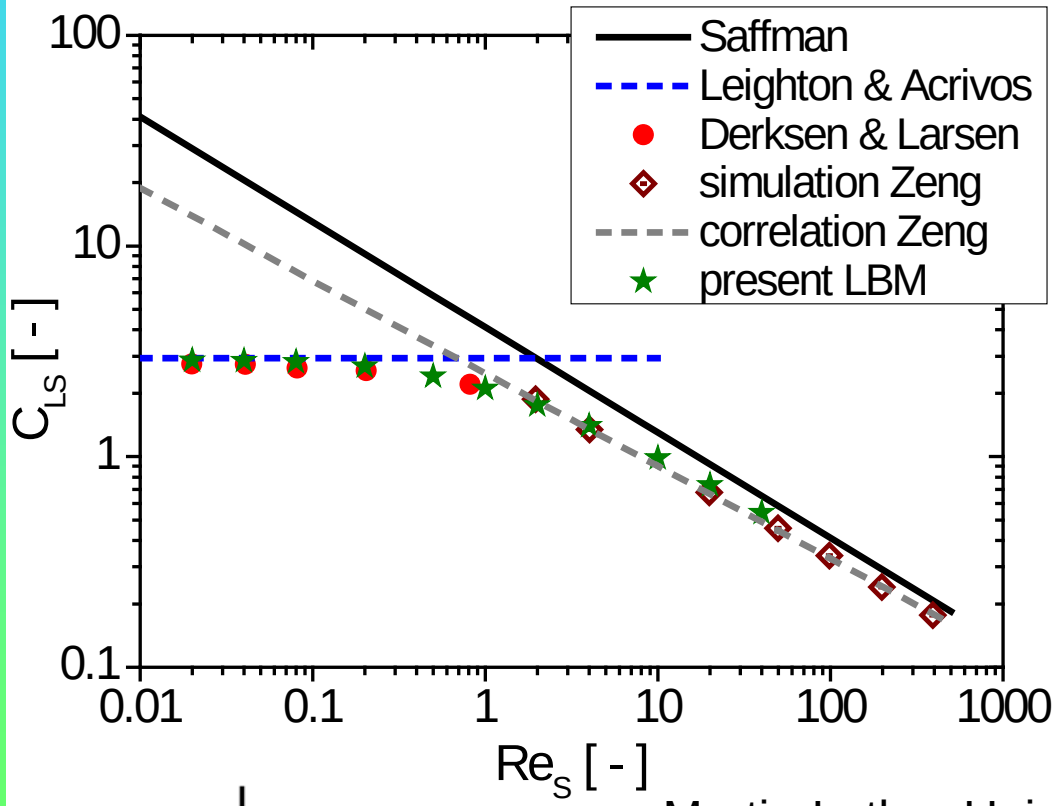

$$Re_S = \frac{\rho\, D_P\, G}{\mu} = 0.02$$

Selected domain size

x/D = 18, y/D = 15, z/D = 15

Simulation Cases

- In the following, simulations of the flow about three different types of particle clusters will be shown.

Nearly spherical clusters consisting of spherical primary particles

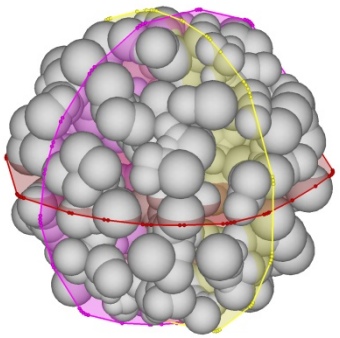

R/a=100

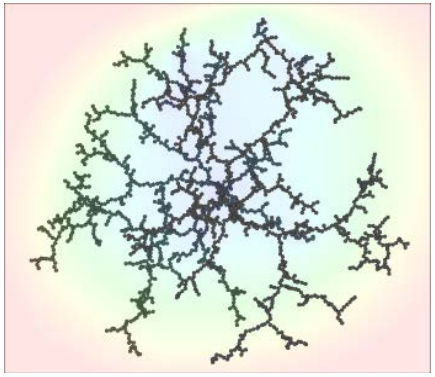

Nearly spherical fractal flocks

Plug, Re=160

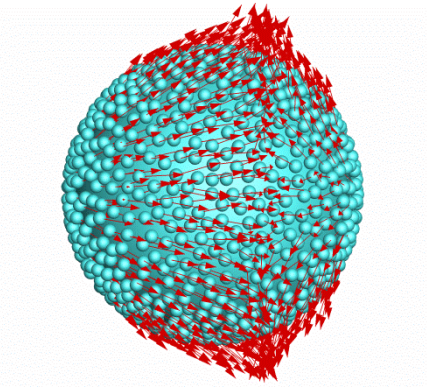

Carrier particle covered with micron-sized powder

Agglomerate Generation

- **Agglomerate generation based on random growth plus design specifications**
  - **creation by definition of:**
    - number and size distribution of primary particles
    - optional sintering of contact points
    - morphological type
      (*dendritic*, *spherical clusters*, *flocks*)
    - target quantity

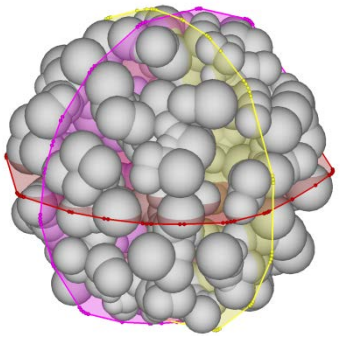

  - **determination of particle characteristics:**
    - equivalent diameters (also used for Reynolds numbers and fluid dynamic coefficients)
    - porosity (e.g. based on convex hull) as main structural parameter
  - **rejection sampling:**
    acceptance or rejection of the created agglomerates based on target parameters

acceptance ← **yes** — $\left| d_{equi} - d_{equi}^{target} \right| \leq \varepsilon$ — **no** → **rejection**

Description of Agglomerate Properties

$\varepsilon_{hull} = 0.61$

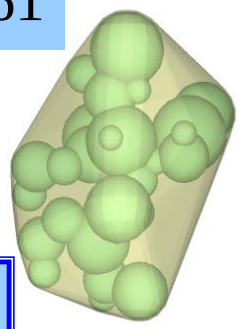

Compact agglomerate with 30 primary particles

☞ **Characteristic properties of agglomerates:**

- Volume, surface, volume specific surface area
- Convex hull volume
- Aggregate density
- Volume equivalent diameter D_{VES}
- Outer radius R_o
- Gyration radius:

$$R_g = \sqrt{\frac{1}{N}\sum_{i=1}^{N}\left|\vec{r}_s - \vec{r}_i\right|^2}$$

- Porosity:

$$\varepsilon = \frac{V_v}{V_{hull}} = \frac{V_{hull} - V_p}{V_{hull}}$$

- Sphericity:

$$\psi = \frac{S_{VES}}{S_{Agg}}$$

- Fractal dimension:

$$m(r) \approx r^{D_f} \qquad 1 < D_f < 3$$

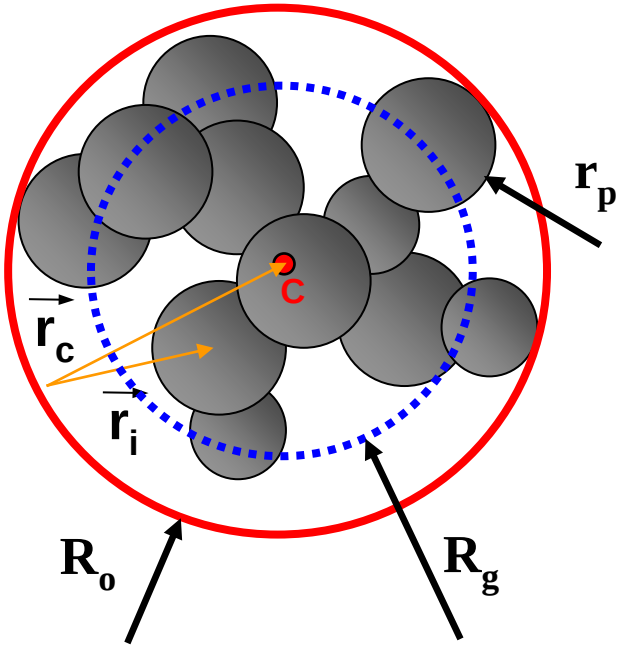

Conditions for the Simulations

☞ **Simulation of 3D-flow around porous spherical agglomerates:**

- **variation of morphology and mean porosity:**
  - ***group G1, G2*:** **spherical clusters with porosity between 30 and 80 %**
    G1: 5 – 10 cells per PP; 2 million cells, 4 FR
    G2: 6 cells per PP; 2 million cells, 4 FR
  - ***group G3*:** **fractal flocks with porosity larger than 90 %**
    1 – 2 cells per PP; 5 – 6 million cells; 2 – 3 FR
- **variation of particle Reynolds number and reference parameters**
- **reference simulation for rigid sphere for wall effect correction**

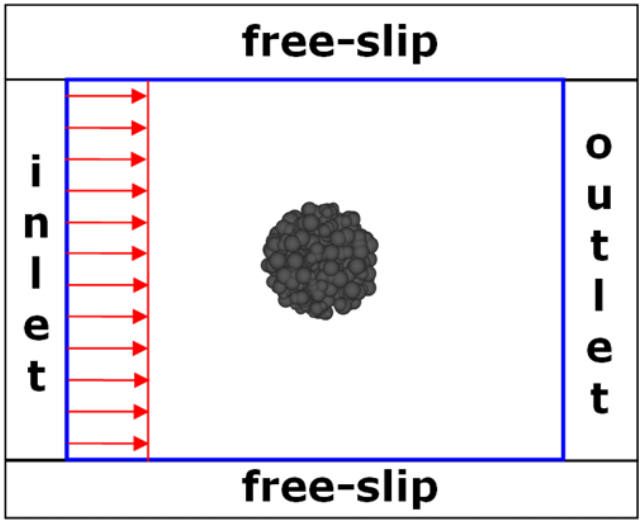

Schematic plot of numerical domain

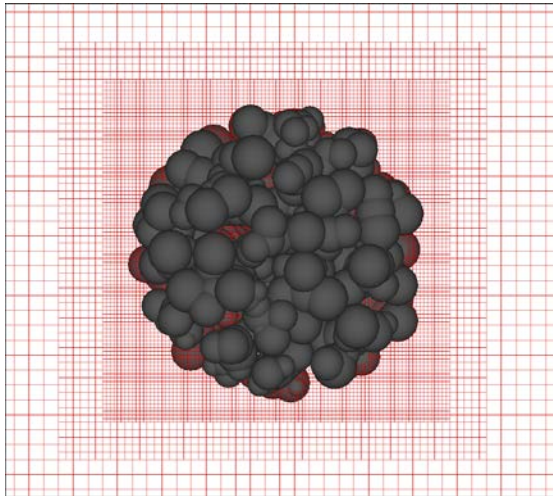

Local grid refinement in the immediate vicinity of the agglomerate

Flow About Spherical Clusters 1

Clusters G1 and G2

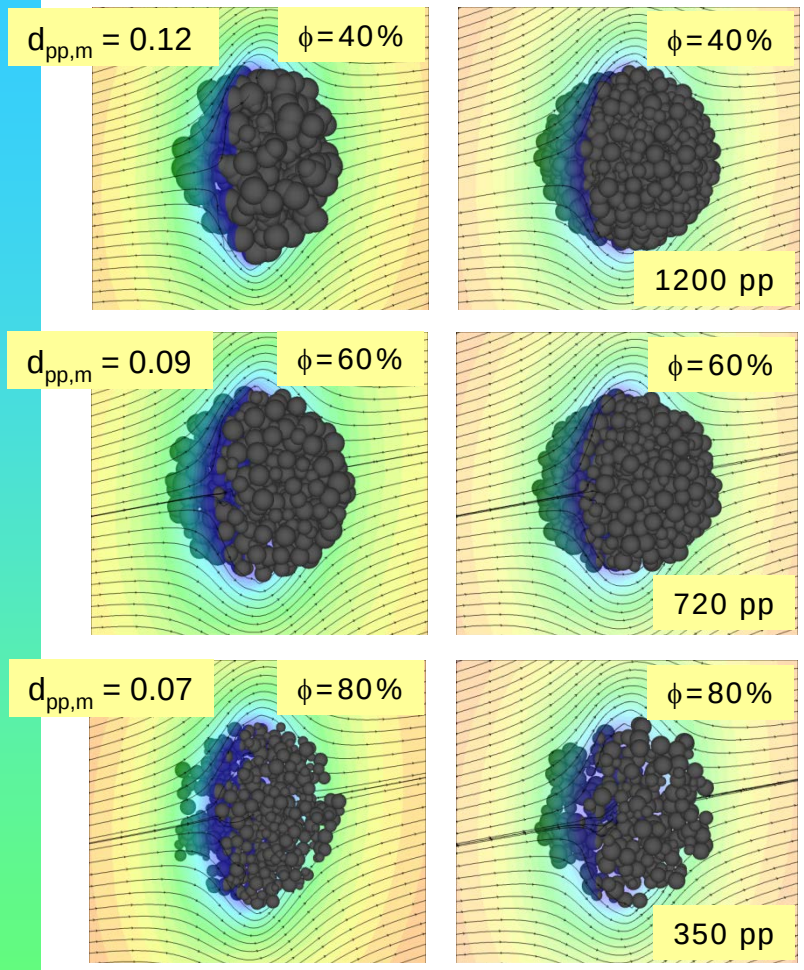

Flow field around particles at Re=0.3

- ⇨ particle size distribution (± 0.4 D_{mean}), sintering at contacts (0.15 to 0.50 D_{mean})
- ⇨ variation of mean porosity: 30 ... 80 %
- ⇨ ***G1: variation of mean primary particle size; constant particle number: 500***
- ⇨ ***G2: constant mean primary particle size particle number: 350 ... 1400***

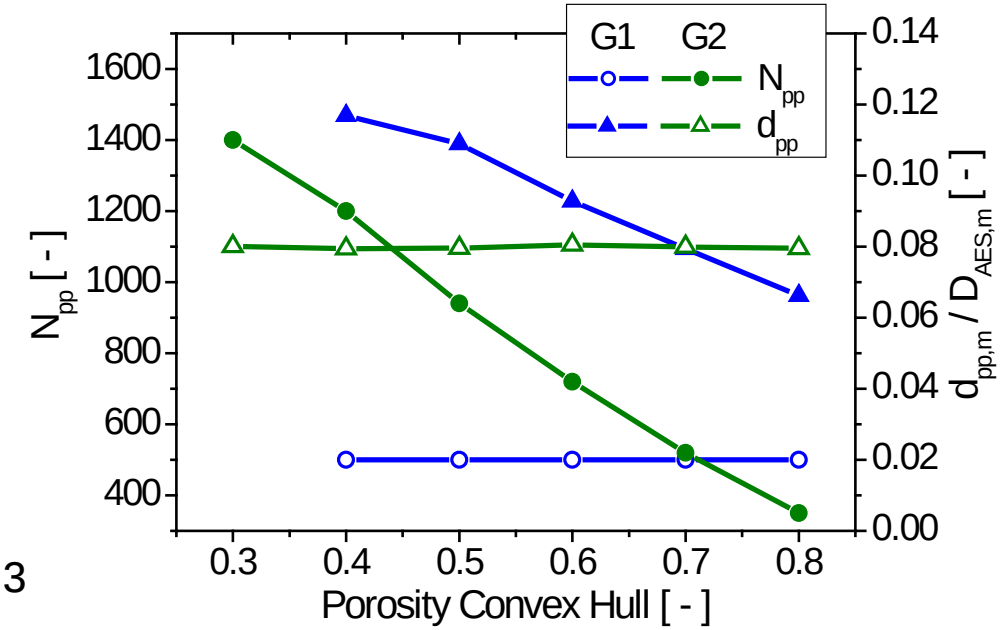

Flow About Spherical Clusters 2

⌦ **Dependence of drag on agglomerate structure (G1 & G2; Re = 0.3):**

- **With the volume equivalent sphere the drag on the agglomerates cannot be described properly**
- **The drag of the agglomerates is lower than the area equivalent sphere**
- **Slight decrease of drag with increasing porosity (drop of 4 – 9 %)**
- **The decrease of drag for low porosity of G1 is related to structural differences (R_g, D_f)**

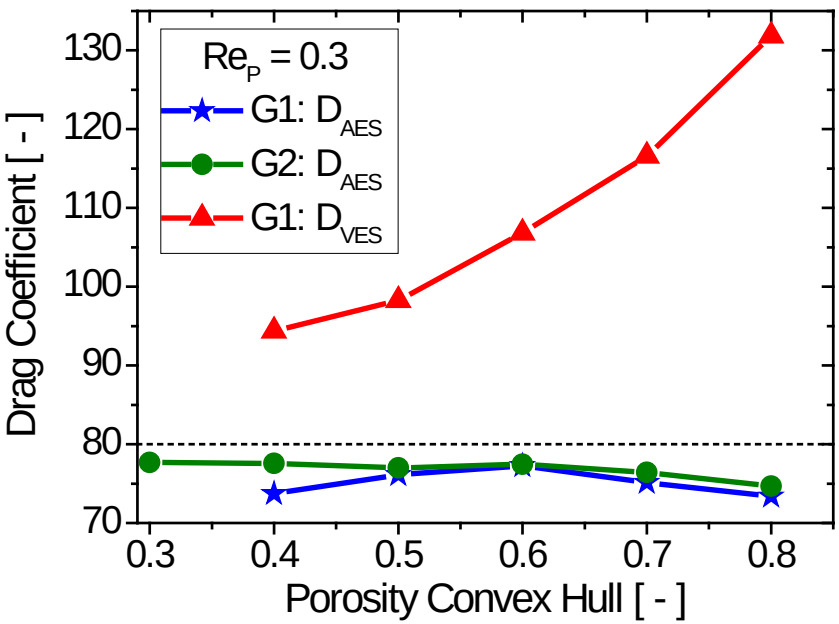

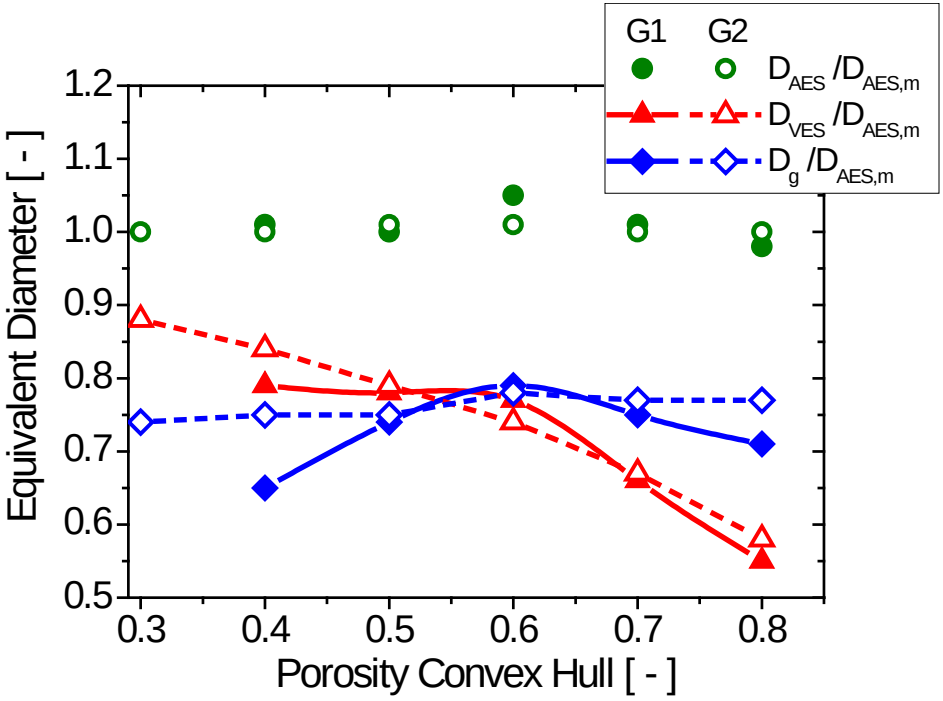

Flow About Spherical Clusters 3

- **Structural effects on radius of gyration and fractal dimension Particle (G1)**

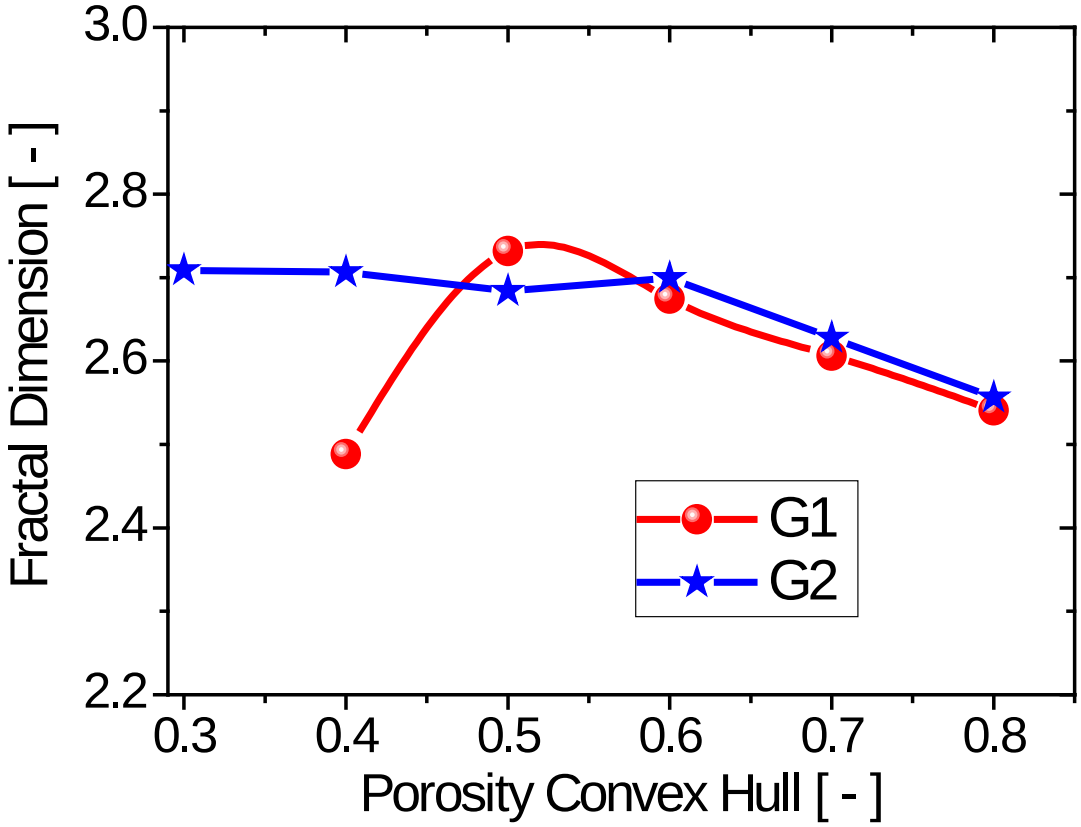

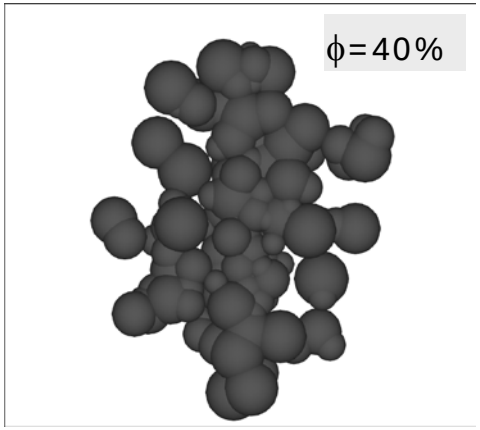

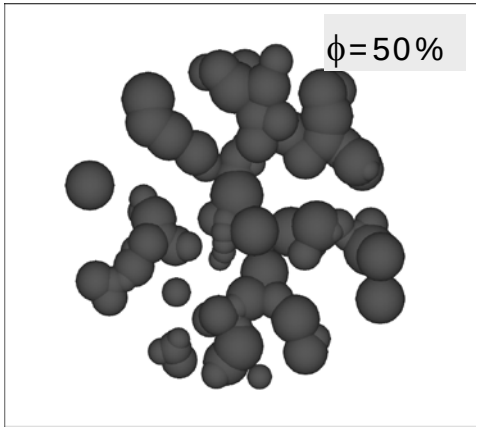

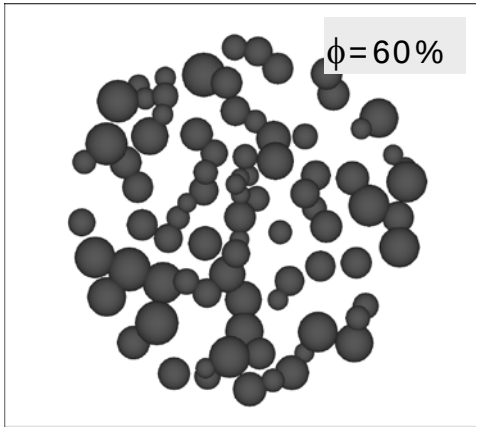

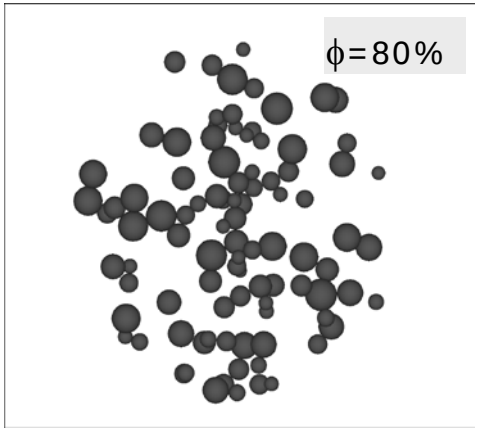

Spherical Flocks 1

- **Investigation of fractal agglomerates (flocks of G3) with different morphology:**
  - ☞ **basis: publication of Vanni (2000):**

    "Creeping flow over spherical permeable aggregates" [Chemical Engineering Science 55, 2000, 685-698]
    - **aggregates with fractal structure: radially varying solids volume fraction and permeability (spherical symmetry)**
    - **assumptions: continuous porosity function, no local heterogeneities**
    - **Stokes equation for external flow and Brinkman equation for internal flow**
  - ☞ **Variation of diameter ratio R/a and fractal dimension D_f**

Diameter ratio	Fractal dimension		Particle number	Solid fraction	Porosity	
R / a	D_f	D_f*	N_{pp}	1 - ϕ	ϕ	ϕ*
50	1,5	1,5	145	0,001	0,999	0,999
50	1,8	1,8	611	0,005	0,995	0,995
50	2,1	**2,2**	2434	0,019	0,981	0,981
50	2,4	**2,6**	9356	0,075	0,925	**0,930**
10	1,8	1,8	34	0,034	0,966	**0,971**
100	1,8	1,8	2127	0,002	0,998	0,998

$$N_{pp} = C_s \left(\frac{R}{a}\right)^{D_f}$$

$$C_s = 0.414\, D_s\text{-}0.211$$

$$\bar{\varphi}(R) = C_s \left(\frac{R}{a}\right)^{D_f - 3}$$

*** Simulated agglomerates**

Spherical Flocks 2

Clusters of group G3 with constant $D_f \approx 1.8$

- **Mono-disperse, point contacts, constant primary particle size**
- ***variation of R/a: 10, 50, 100 (agglomerate outer radius/primary particle radius)***
- ***variation of particle number: 34 … 2127***

R/a=10

R/a=50

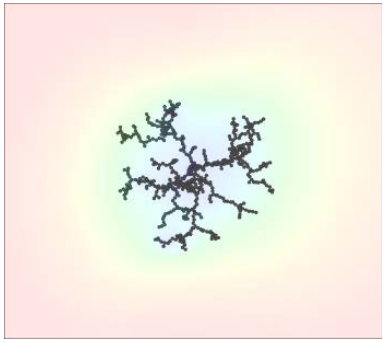

R/a=100

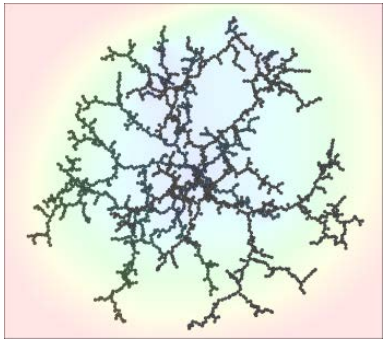

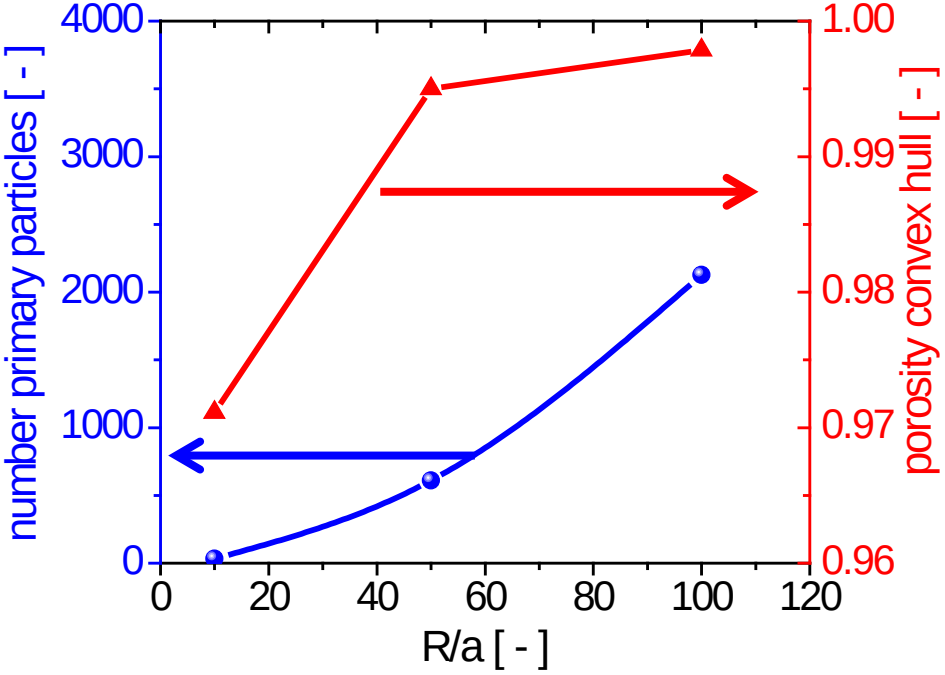

Spherical Flocks 3

Drag of G3 with constant $D_f \approx 1.8$ at Re = 0.1

- **Influence of size ratio R/a (comparison with Vanni 2000):**
  - **Re and drag coefficient are referred to the enwrapping sphere**
  - **As a result of the inhomogeneous porosity distribution within the agglomerate the simulated drag is lower than predicted by Vanni**

R/a=10

R/a=50

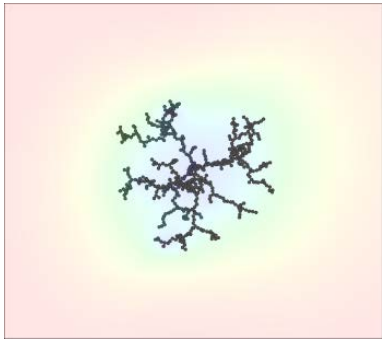

R/a=100

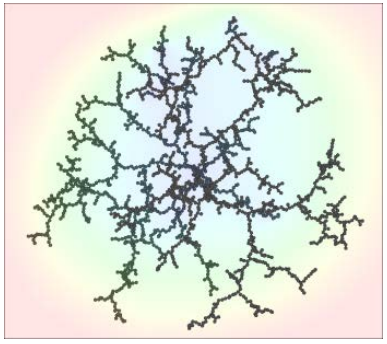

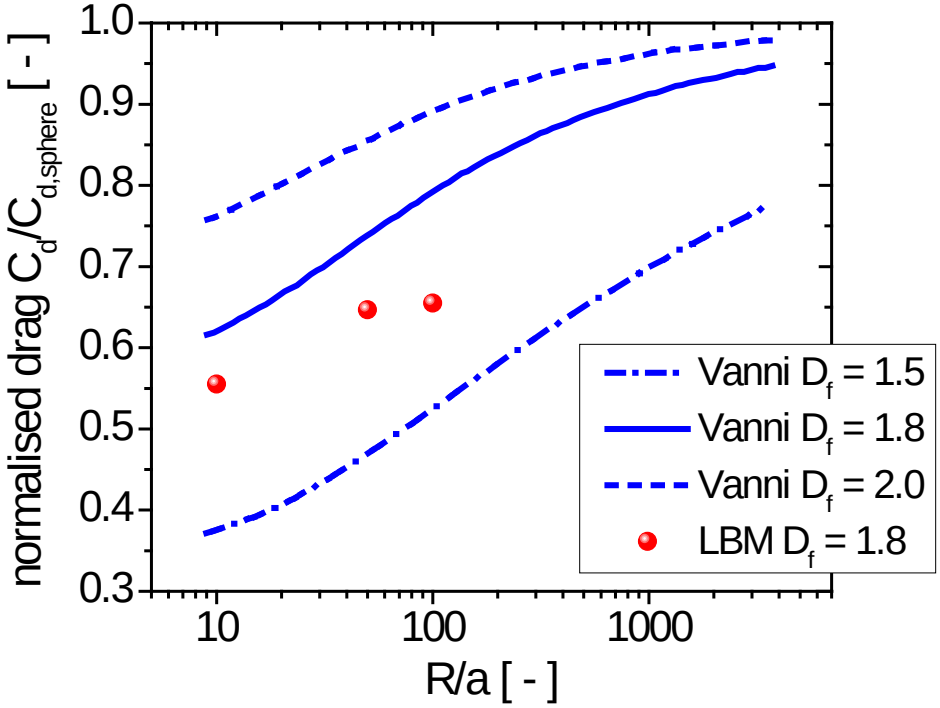

Spherical Flocks 4

Clusters of group G3 with constant R/a = 50

- **Mono-disperse, point contacts, constant primary particle size**
- ***variation of D_f: 1.5, 1.8, 2.2, 2.6***
- ***variation of particle number: 145 … 9356***

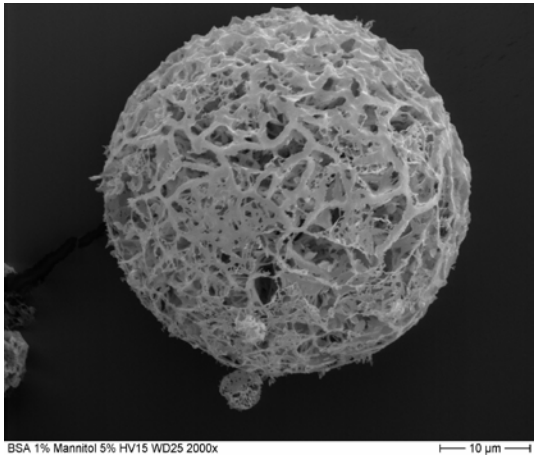

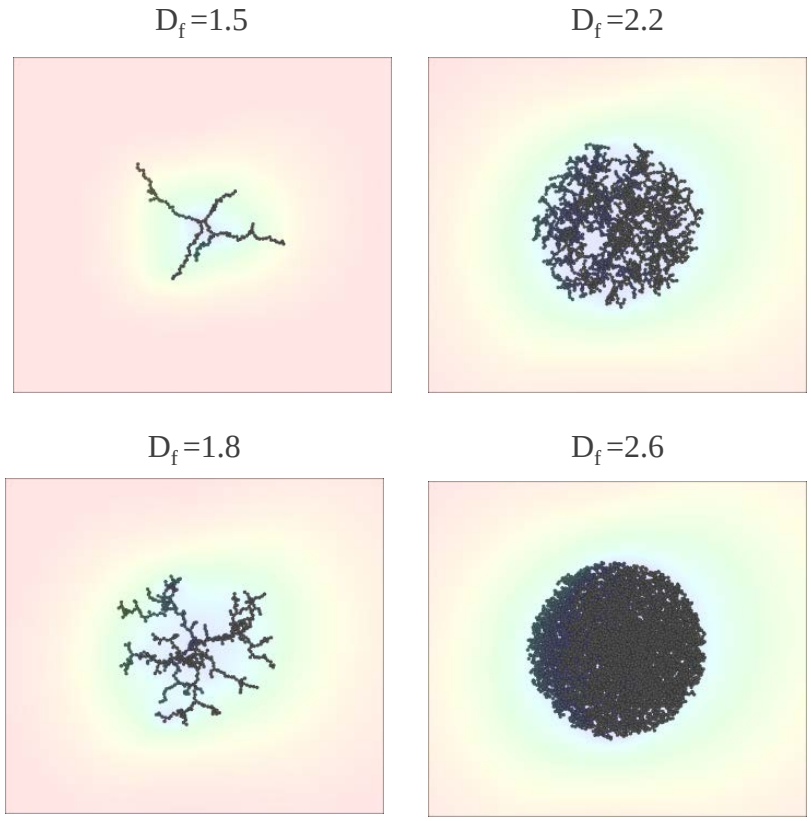

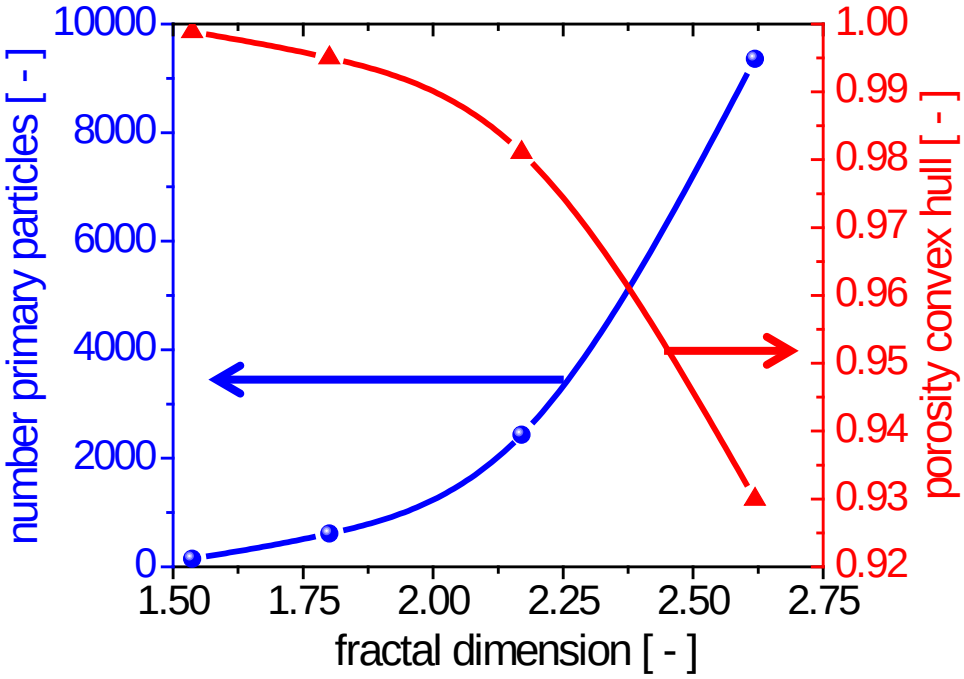

Spherical Flocks 5

Drag of G3 with constant R/a = 50 at Re = 0.1

- **Influence of fractal dimension D_f:**
  - Re and drag coefficient are referred to bounding sphere
  - Drag coefficient decreases with reducing fractal dimension; differences with the theory of Vanni (2000) due to inhomogeneity in porosity

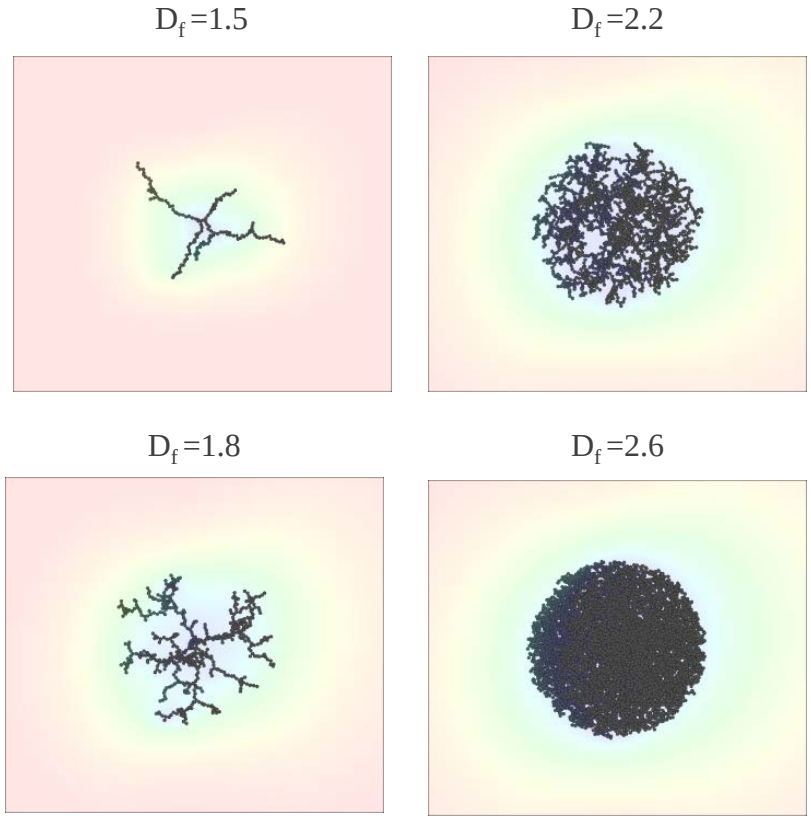

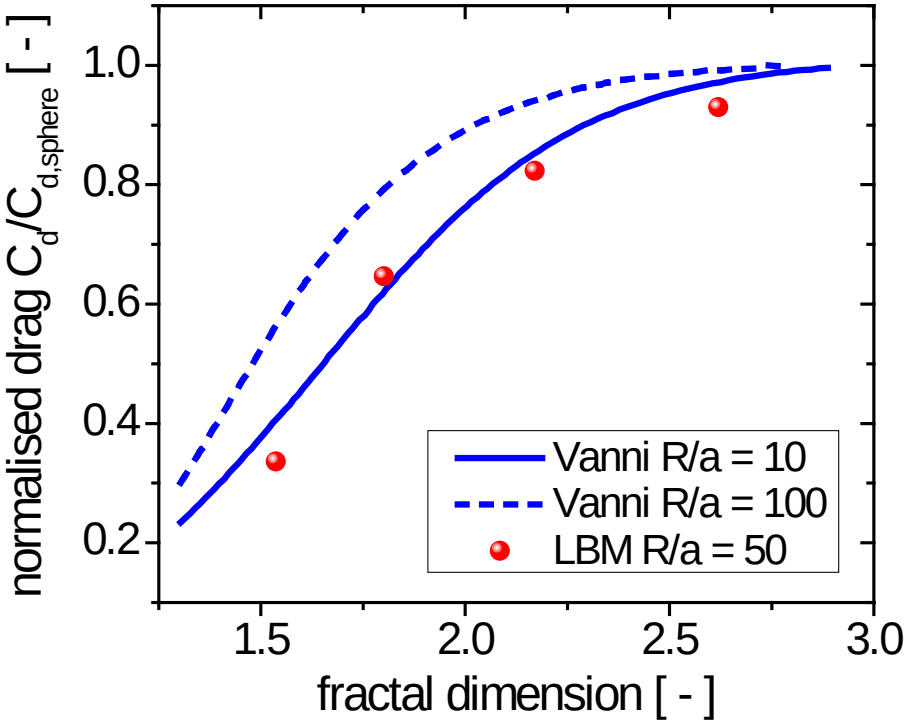

Simulation Conditions Particle Cluster 1

- For the inhalation of fine drug powders below 5 μm, carrier particles (100 μm) are coated with the drug particles.
- Within the inhaler the drug powder needs to be detached from the carrier through fluid stresses and wall impacts.
- The flow conditions considered for the LBM mimic the conditions experienced by a carrier particle in an inhaler.

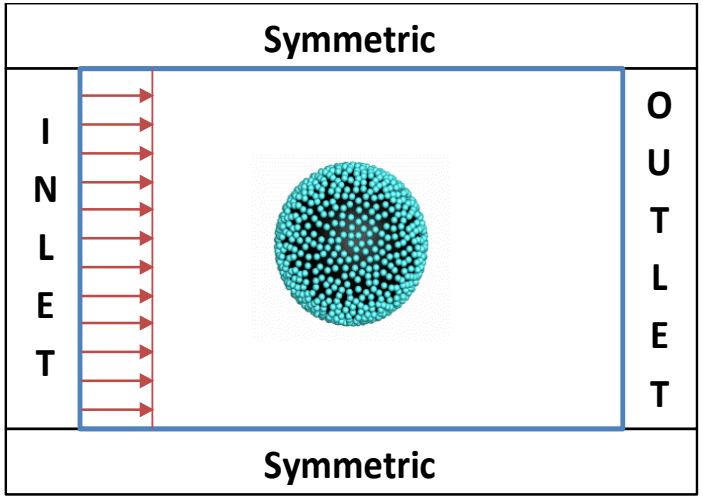

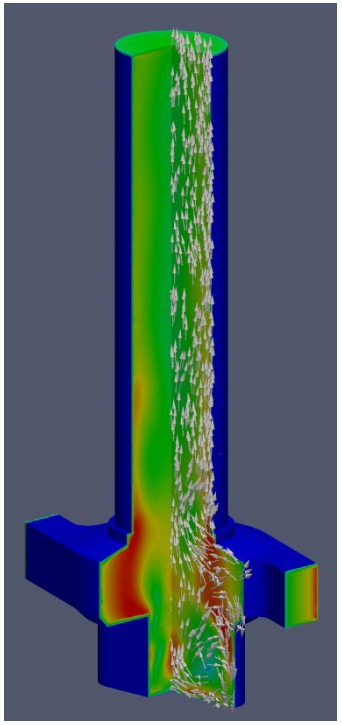

The relevant forces for particle detachment are the normal force acting against the van der Waals adhesion force and the tangential force acting against friction force.

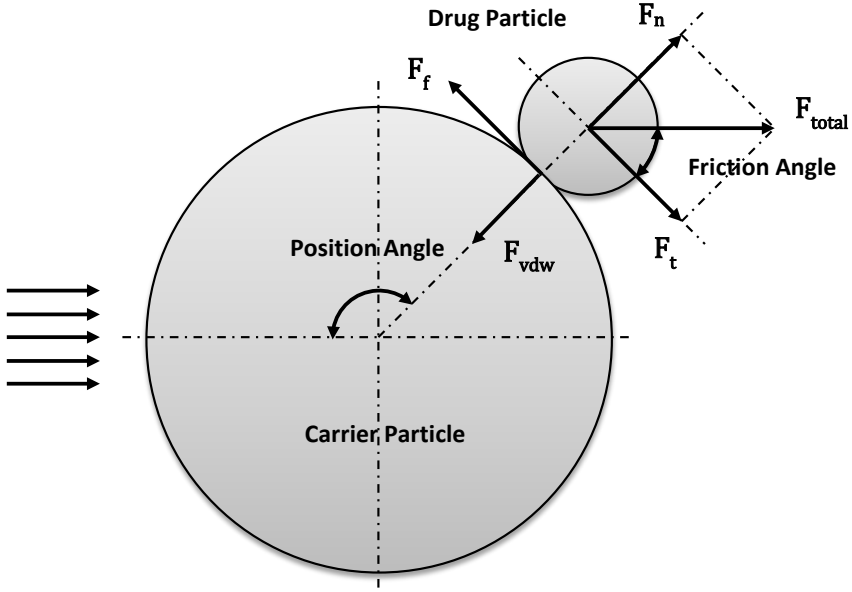

Simulation Conditions Particle Cluster 2

➢ **Validation of drug particle resolution:**

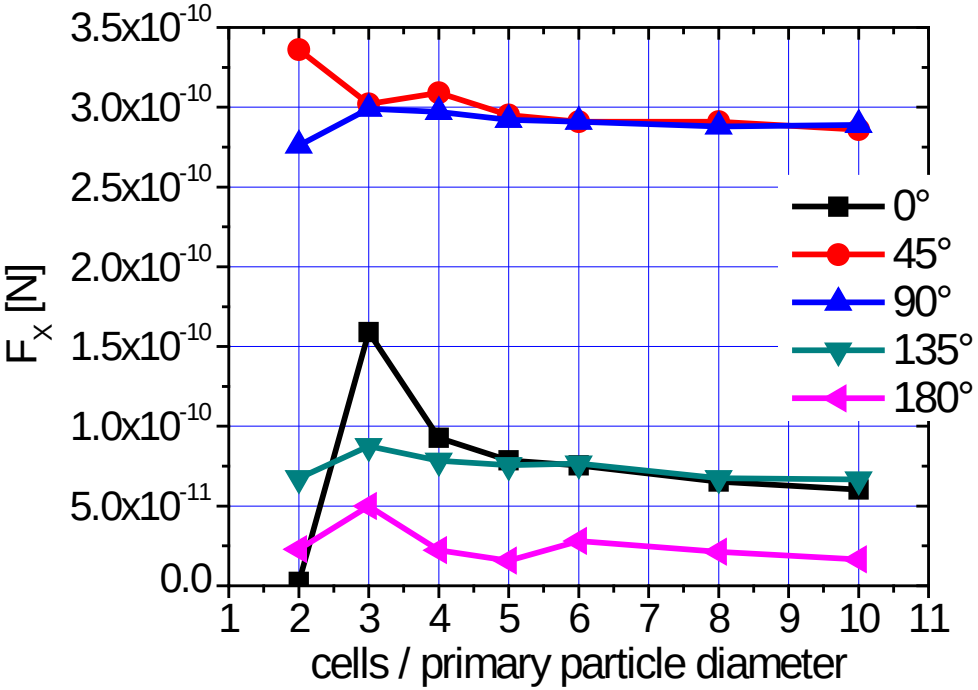

Local grid refinement

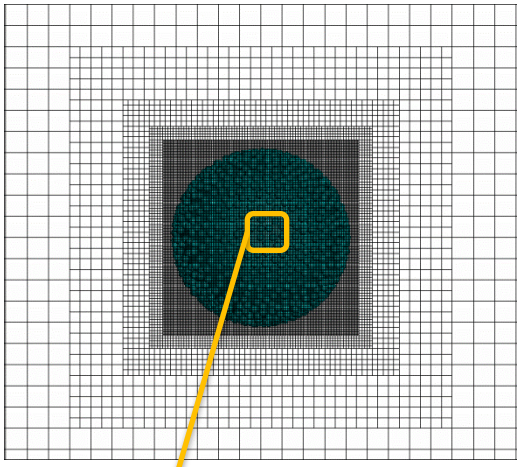

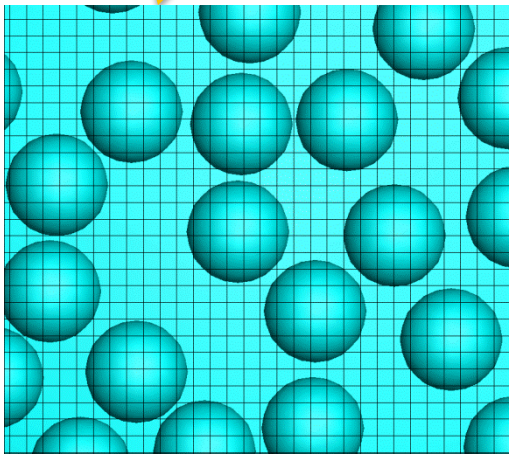

6 Cells per Agent Particle

Simulation Conditions Particle Cluster 3

➢ **Validation of domain size in stream-wise and lateral directions:**

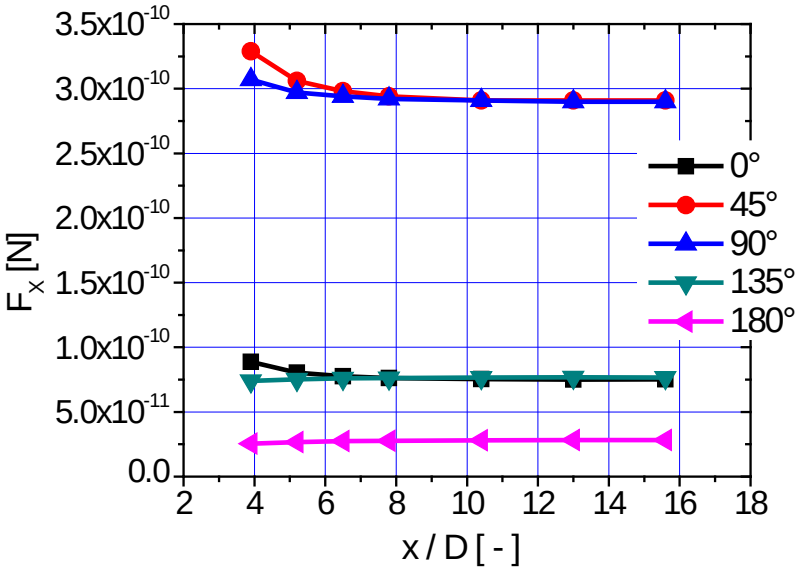

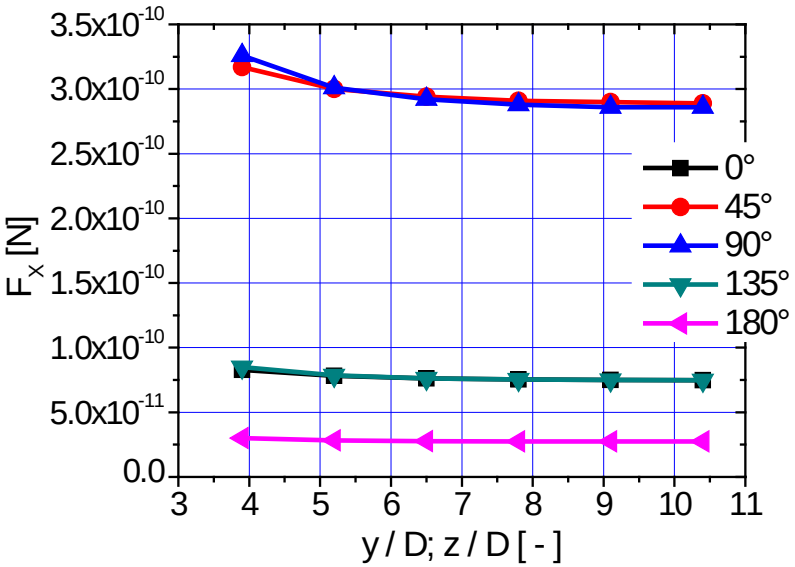

	Stream-wise direction	Lateral directions
Re < 100	$7.8 \cdot D_{carrier}$ $60 \cdot \Delta x_{coarse}$	$6.5 \cdot D_{carrier}$ $50 \cdot \Delta x_{coarse}$
Re > 100	$10.4 \cdot D_{carrier}$ $160 \cdot \Delta x_{coarse}$	$9.1 \cdot D_{carrier}$ $140 \cdot \Delta x_{coarse}$

Plug flow

Present simulation

Re = 16

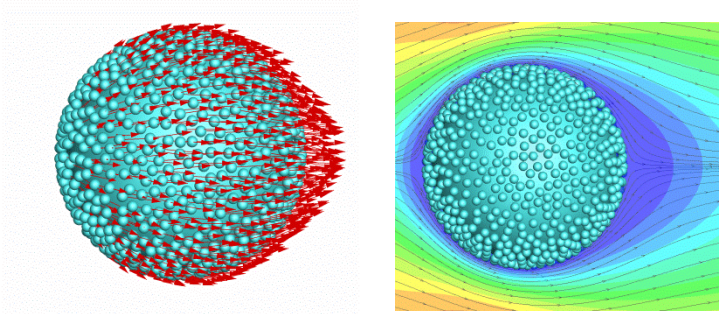

Re = 32

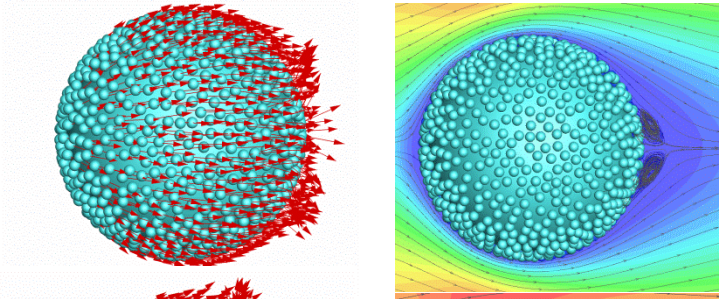

Re = 100

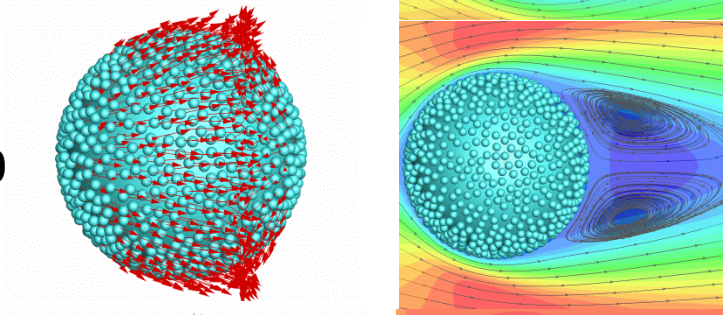

Re = 200

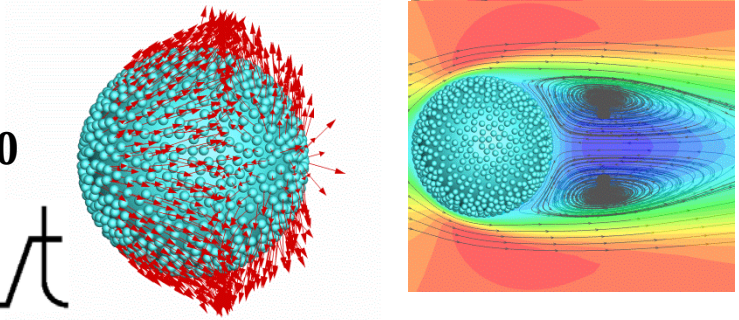

Measurement of S. Taneda

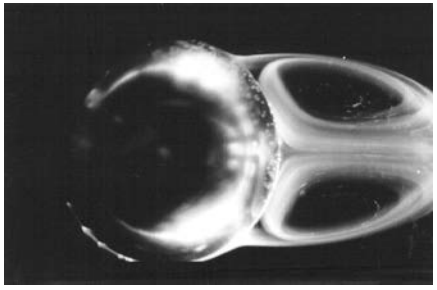

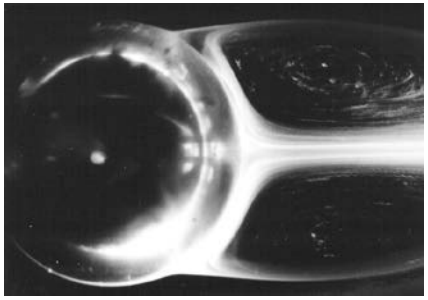

Evaluation of Results

- ☞ **For obtaining reasonable averages of the forces on the drug particle four simulation runs with different random distribution of the fine drug particles.**
- ☞ **Through all data points a polynomial fit is constructed.**

Plug flow, degree of coverage 50%, $D_{drug}/D_{carrier}$ = 5/100

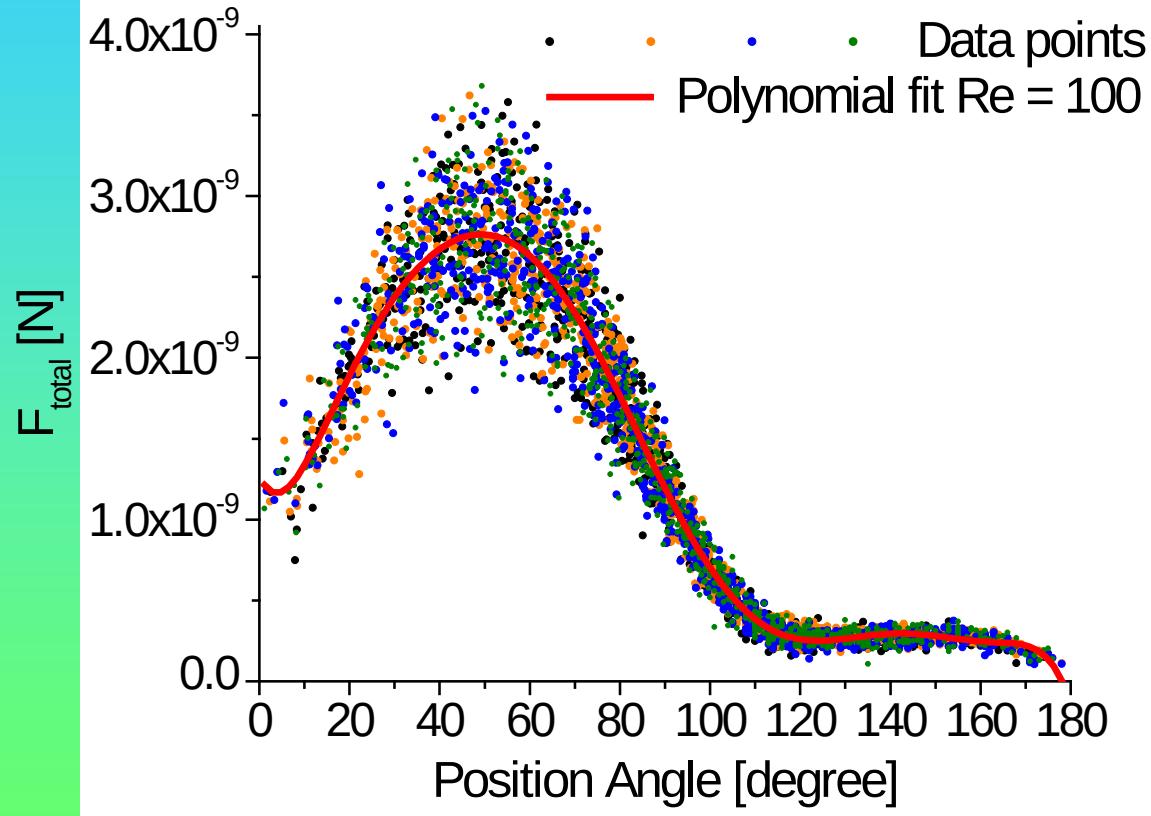

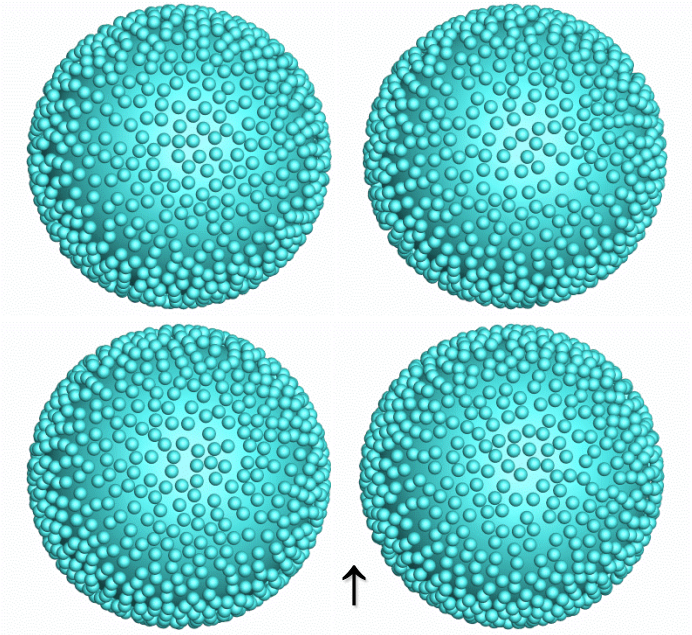

Different drug particle distribution

Effect of Reynolds number

Influence of Reynolds number on normal force distribution

Plug flow, degree of coverage 50%, $D_{drug}/D_{carrier}$ = 5/100

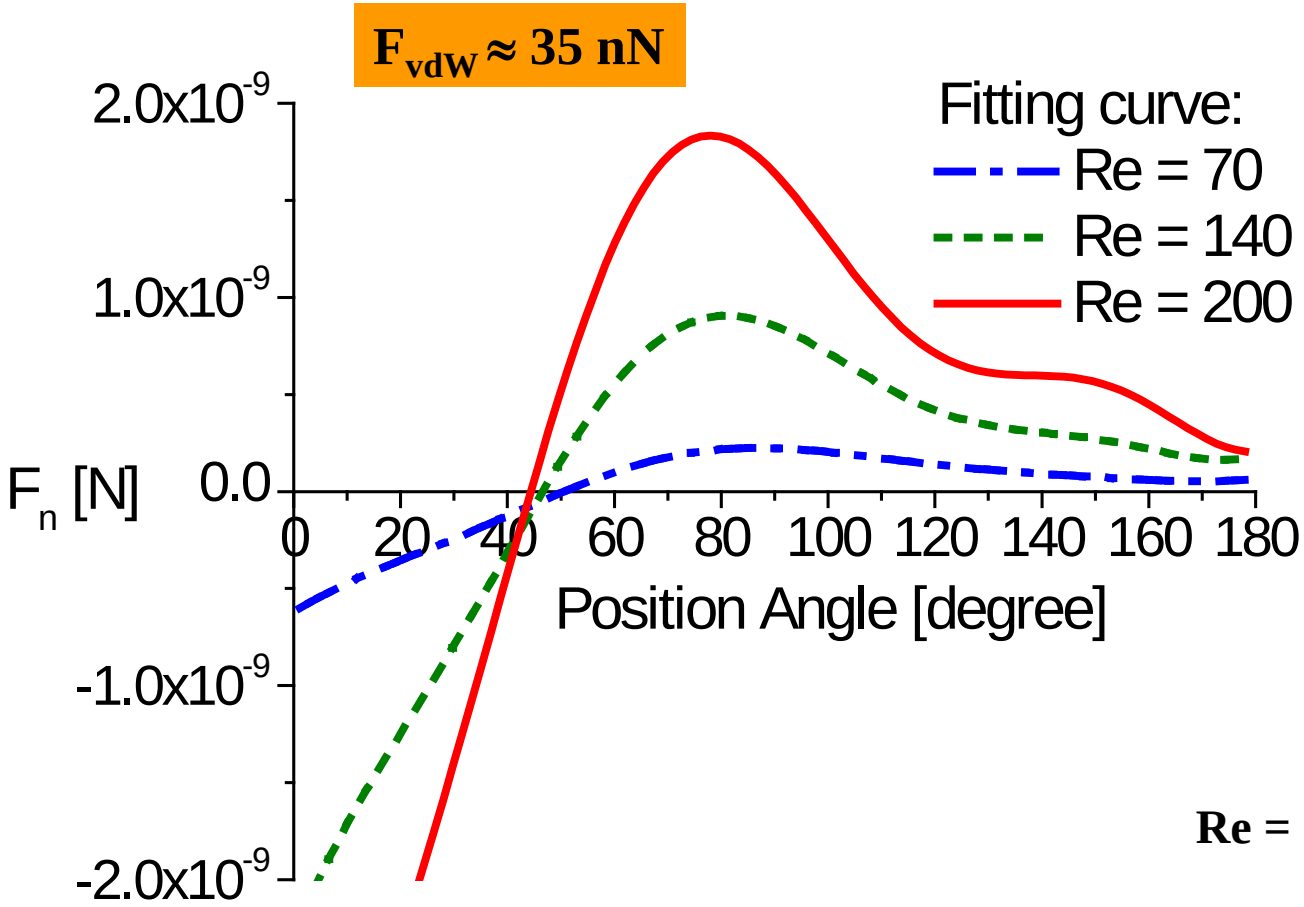

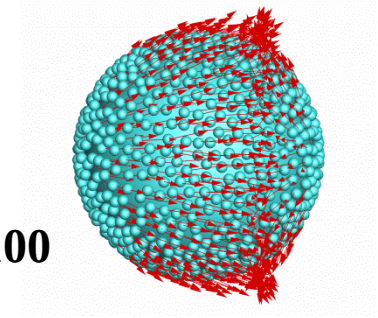

Re = 100

Magnitude and Location of Maximum Normal Force

☞ **Maximum normal force, plug flow, coverage degree 50 %, $D_{drug}/D_{carrier}$ = 5 /100**

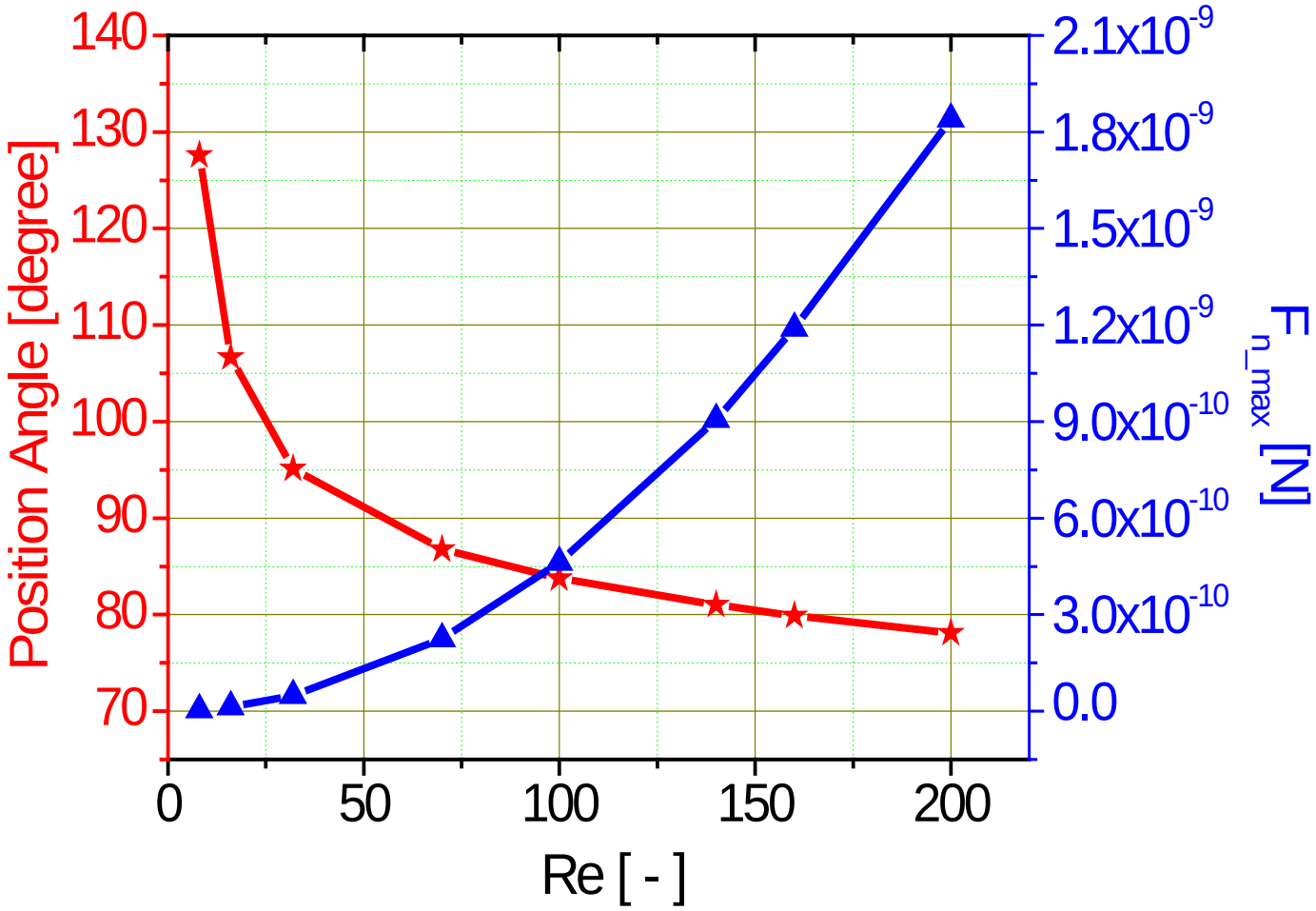

Influence of Coverage Degree

- Influence of the degree of coverage by drug particles on the normal force distribution, plug flow, $D_{drug}/D_{carrier}$ = 5 /100

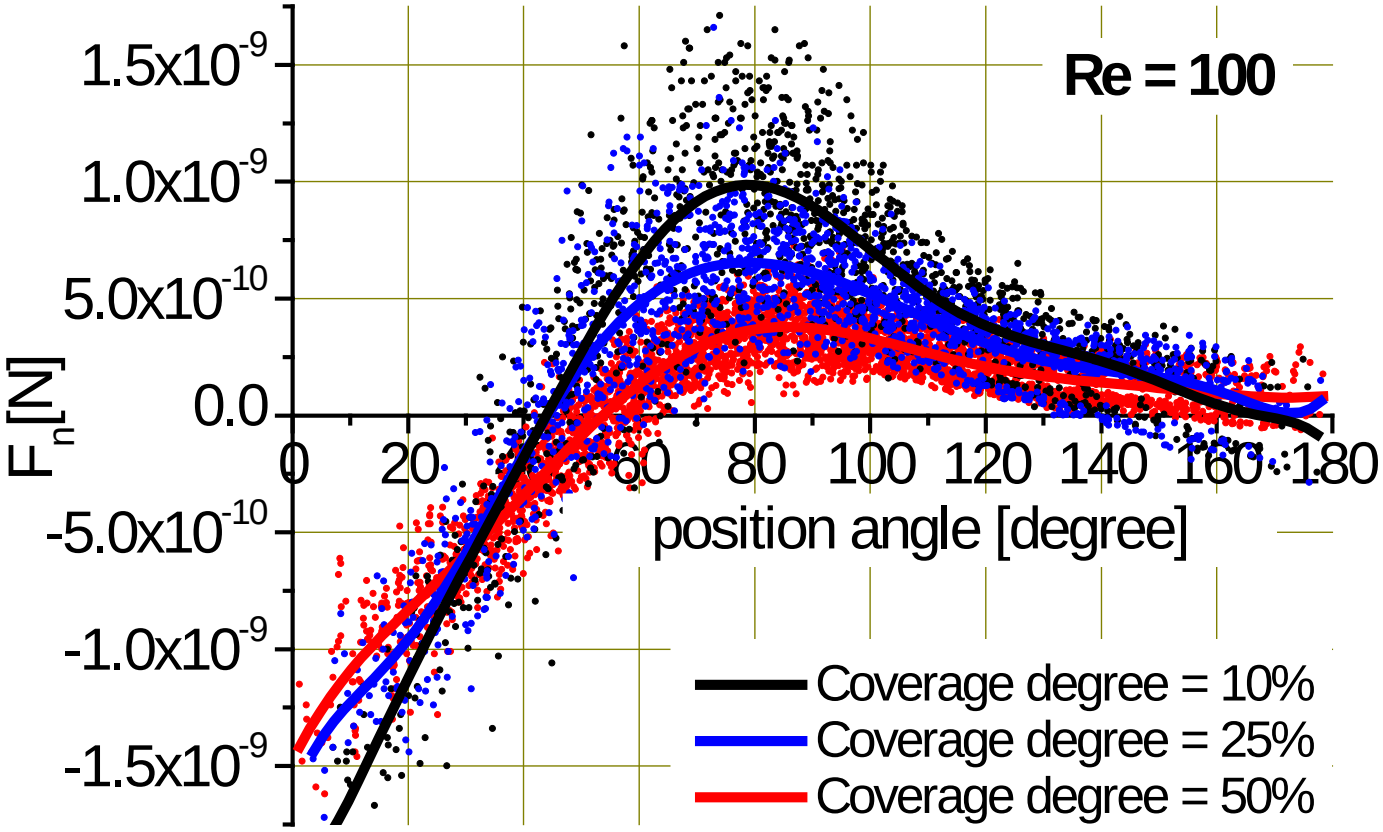

Flow between agent particles

- **For high Reynolds numbers, different coverage degree may have some effect on agent particles. Since there is flow separation in the gap between agent particles. The influence of flow separation will be studied later.**

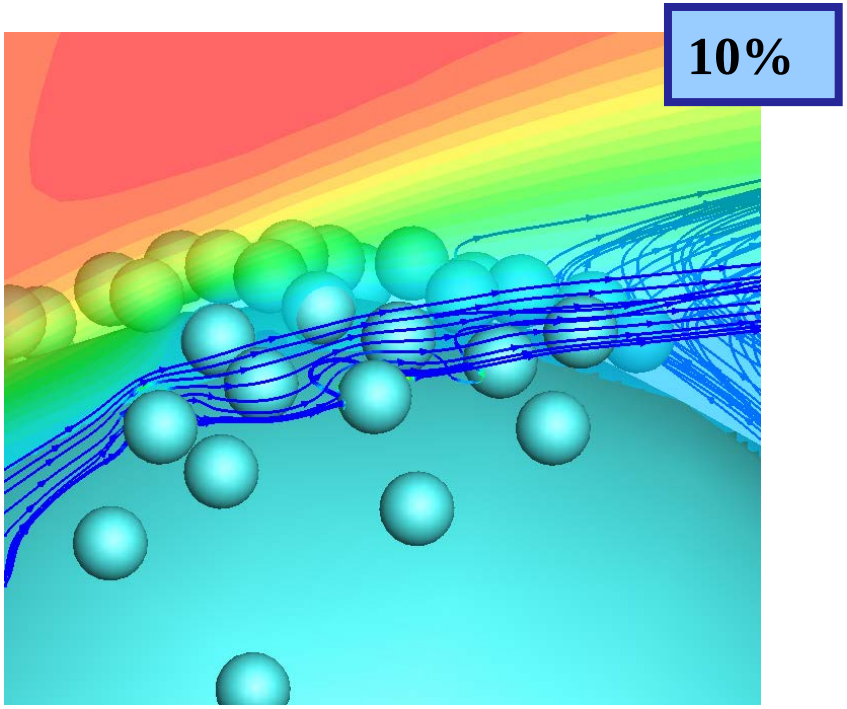

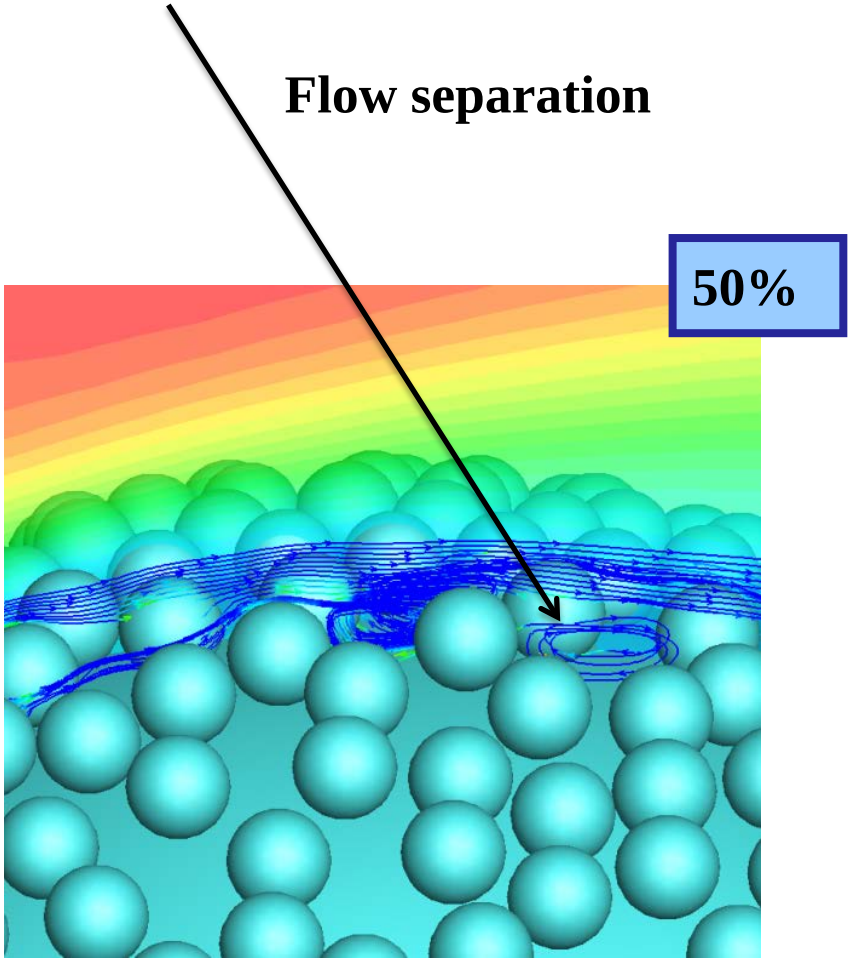

Re = 200

$D_{drug}/D_{carrier}$ = 5 /100

Drag Coefficient for Particle Clusters

- **Comparison of the drag coefficient resulting from present simulation results for a particle cluster with the correlation of Schiller and Naumann (1933) for a sphere (particle diameters $D_{cluster} = D_{sphere} = 110\ \mu m$, coverage degree 10% and 50%, $D_{fine}/D_{carrier} = 5/100$)**

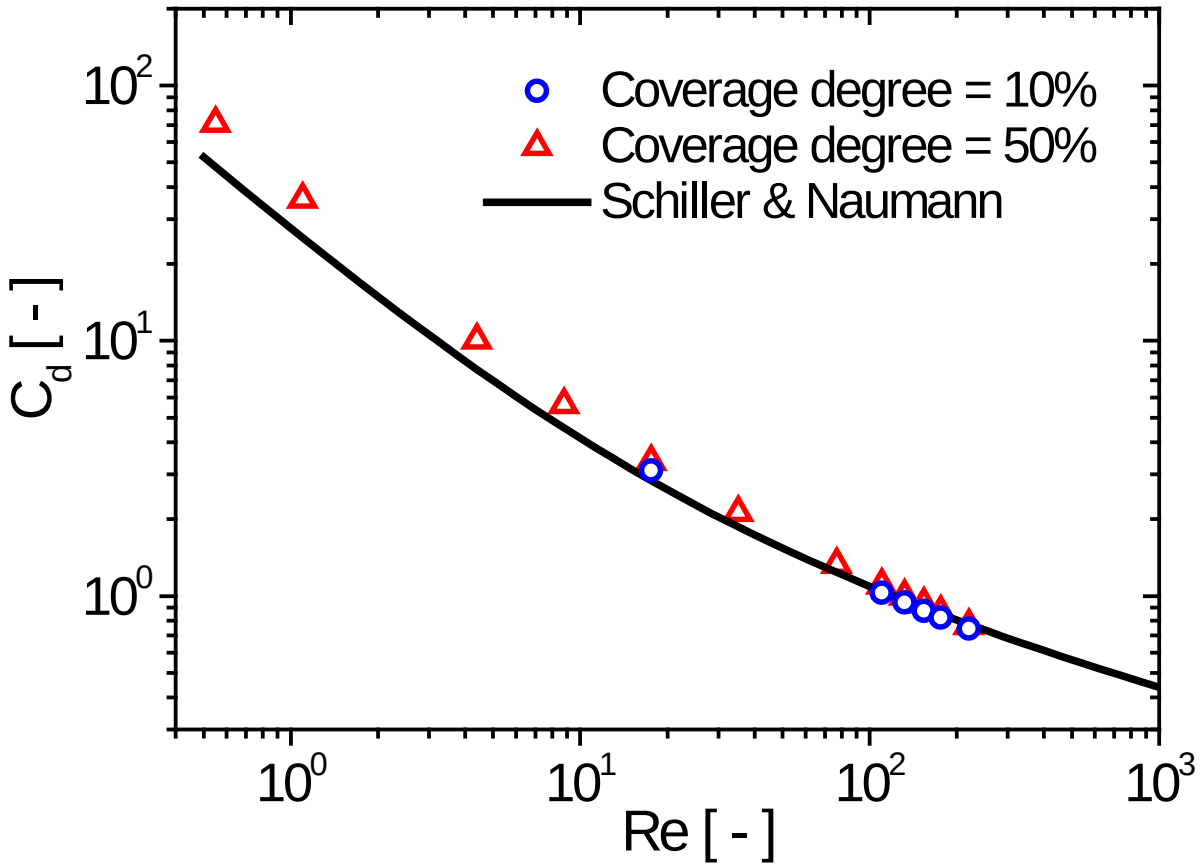

Detachment Probability by Rolling

- **Detachment of drug particles happens through lift-off, sliding and rolling**

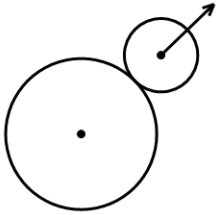

$$F_n > F_{vdW}$$

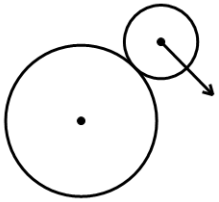

$$F_t > \mu\left(F_{vdW} - F_n\right)$$

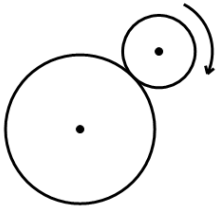

- **Fraction of fine particles to role as a function of Reynolds number for different coverage degree ($D_{fine}/D_{carrier}$ = 5/100, static friction coefficient μ = 0.1, van der Waals force F_{vdW} = 35 nN)**

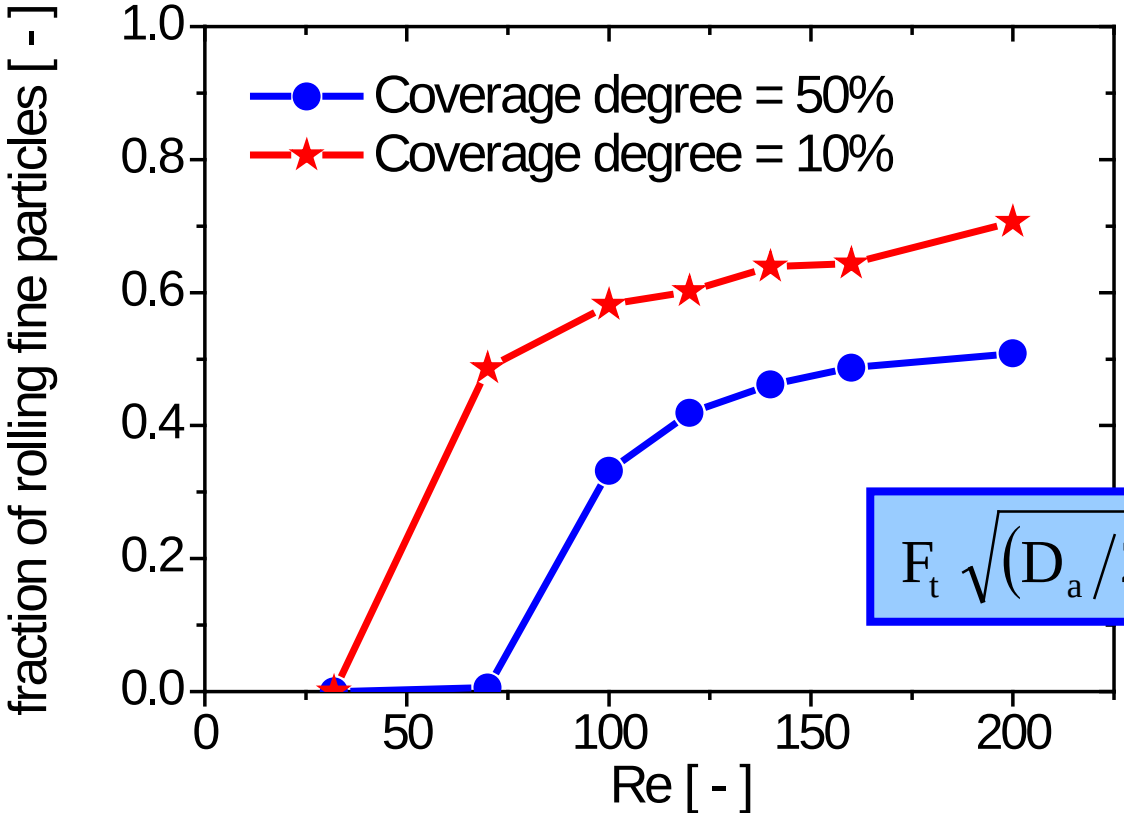

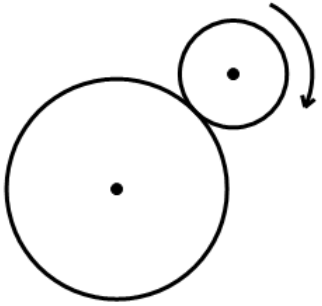

$$F_t \sqrt{\left(D_a/2\right)^2 - a^2} + a\,F_n > a\,F_{vdW}$$

Comparison of Shear and Plug Flow

Plug vs. shear flow, degree of coverage 50%, $D_{drug}/D_{carrier}$ = 5/100

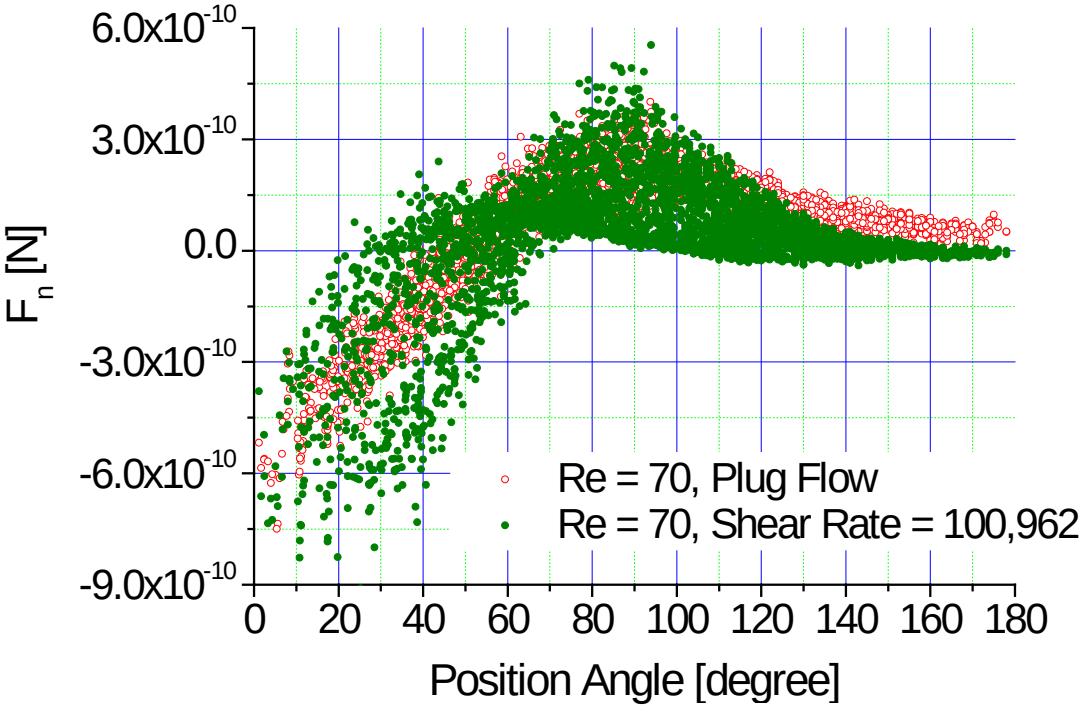

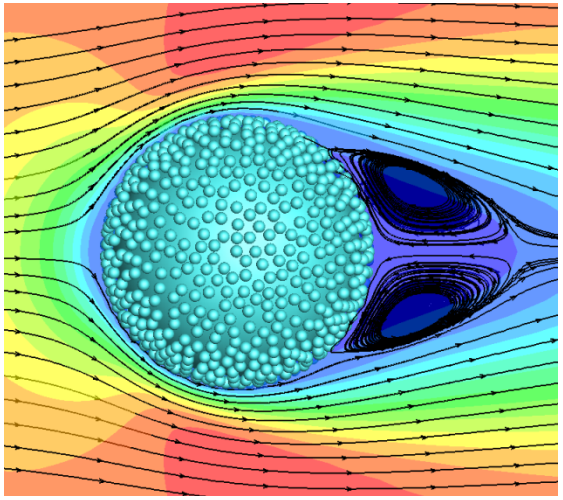

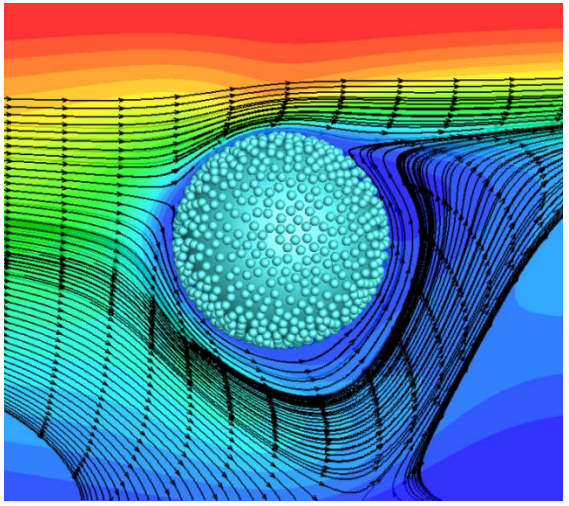

Re = 70

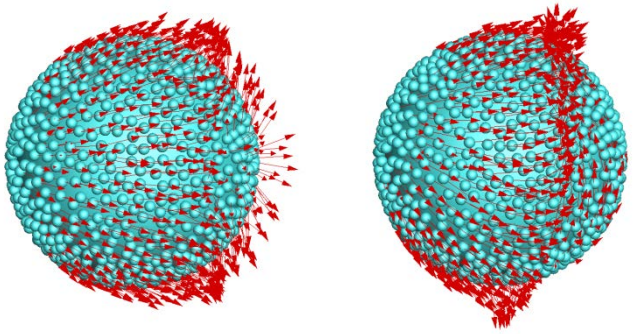

Turbulence Intensity 1

- **Force in x-direction on a single fine particle as a function of time for different turbulence intensity (Re = 70, coverage degree 50 %, $D_{fine}/D_{carrier}$ = 5/100)**

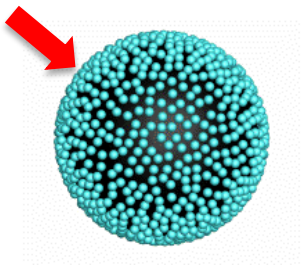

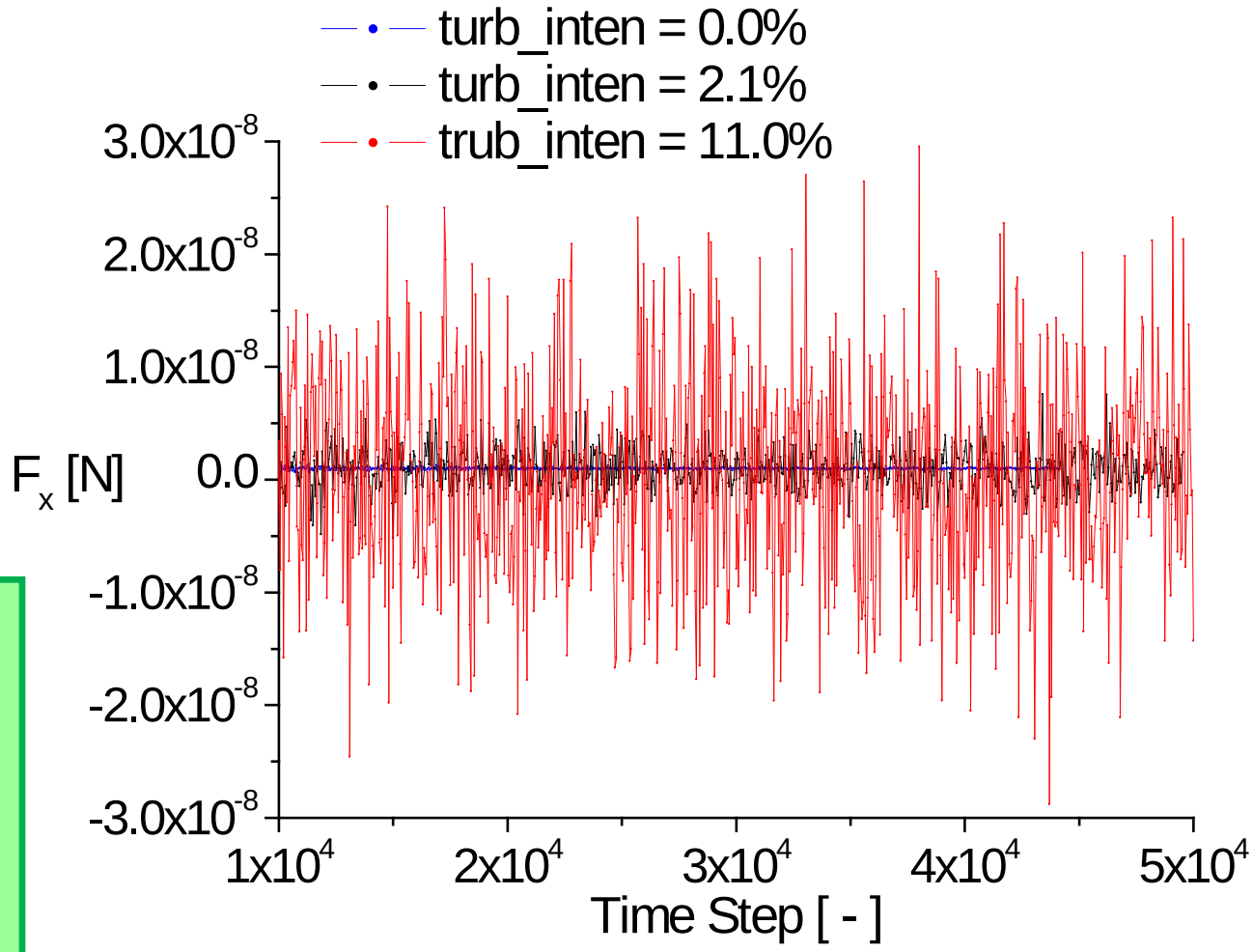

Inflow generation technique based on digital filter, inducing correlation in space and time on the randomly generated data (Klein & Janicka 2003)

Turbulence Intensity 2

- **Magnification of force in stream-wise direction acting on the drug particle for different turbulence intensity**

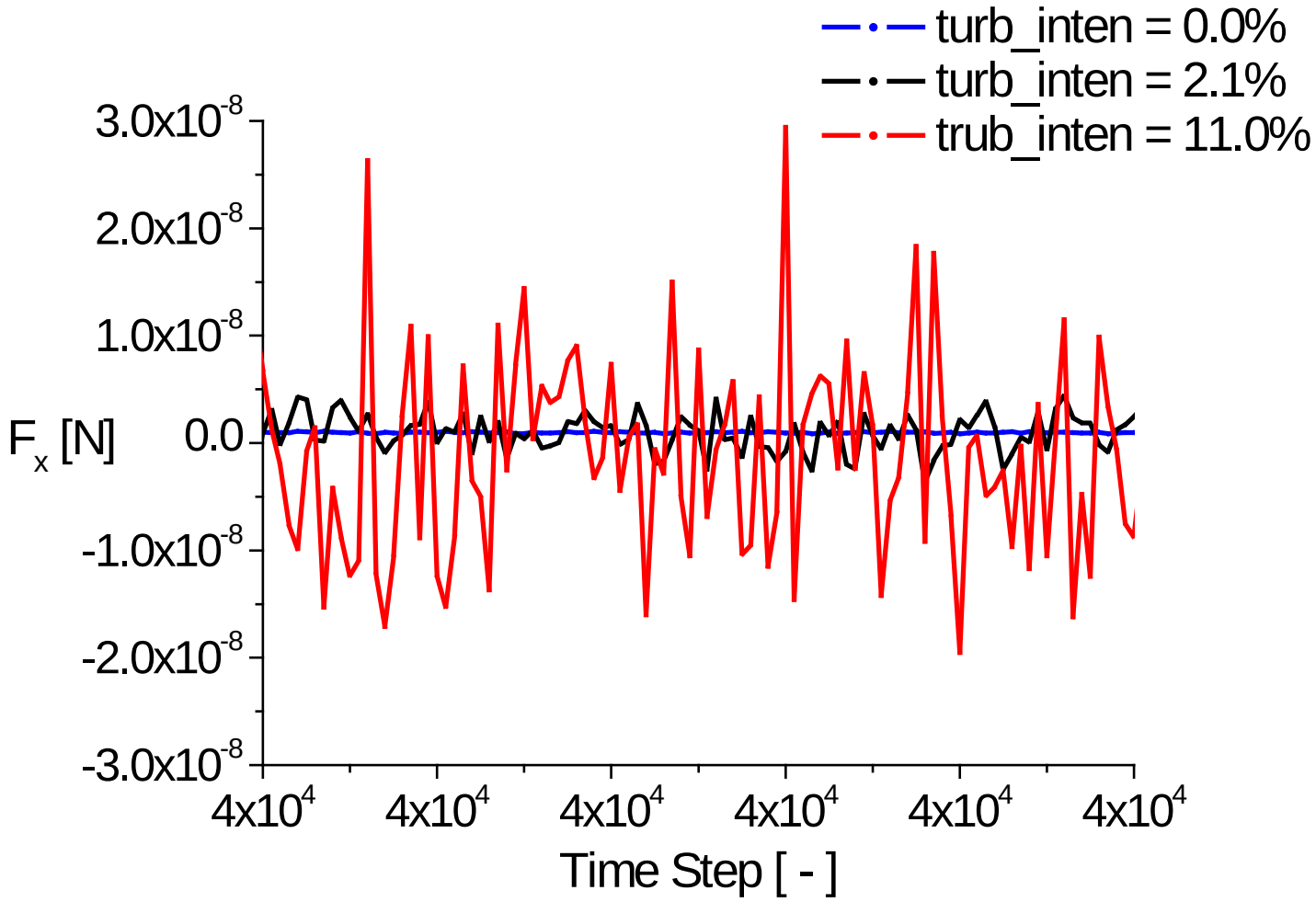

Turbulence Intensity 3

- **Standard deviation of the normal force on the fine particles in dependence of position angle for different turbulence intensity (Re = 70, coverage degree 50 %, $D_{fine}/D_{carrier}$ = 5/100)**

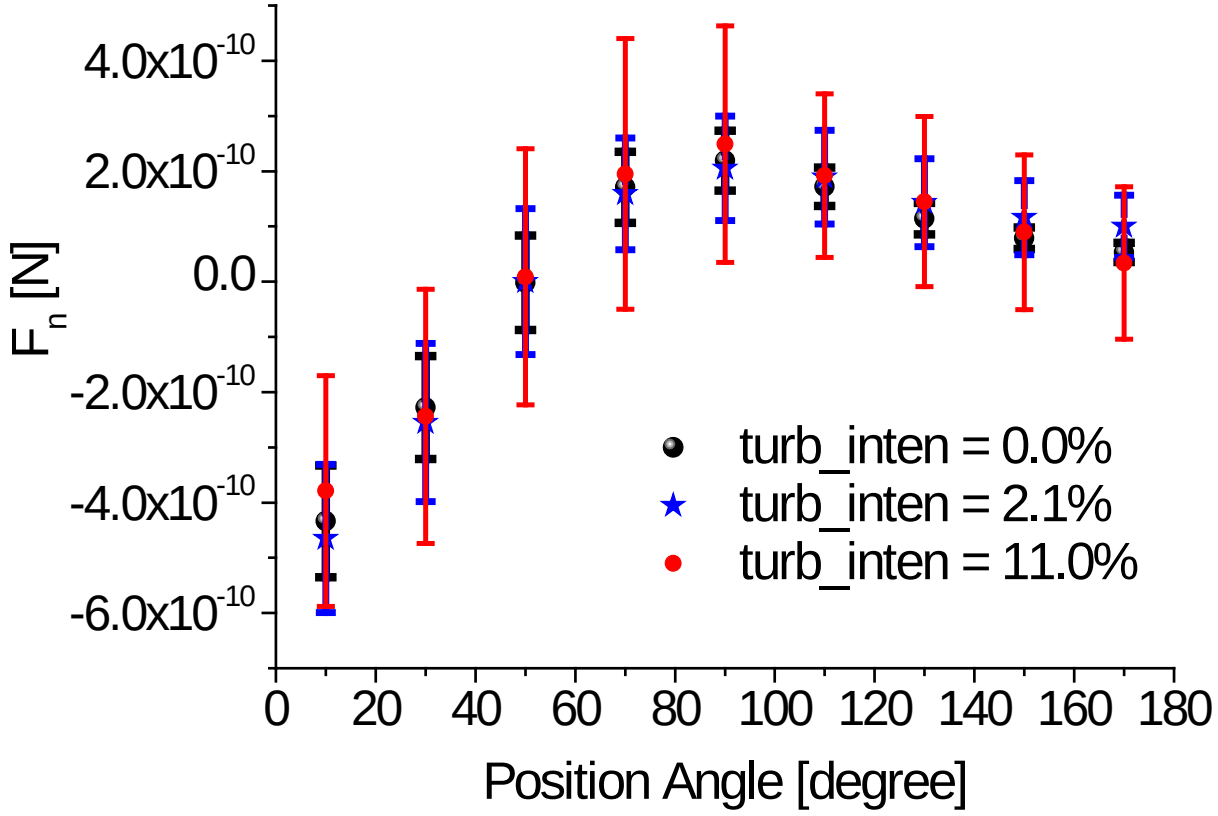

Summary / Conclusions

- **Agglomeration of fine particles and agglomerate transport is an important elementary process in many industrial processes**
- **A numerical calculation of such processes, for example, by the Euler/Lagrange approach requires knowledge about the fluid dynamic behaviour of structured agglomerates**
- **For deriving the resistance coefficients of agglomerates direct numerical simulations were performed by the Lattice-Boltzmann Method**
- **The LBM is a very effective method for calculating the flow about complex bodies and structures, such as agglomerates**
- **For spherical agglomerates it was found that the drag coefficient only slightly decreases with increasing porosity, about 10 %**
- **The results for the spherical flocks are consistent with the data of Vanni, however, some quantitative differences are found which are caused by the real structures (no spherical symmetry) generated for the LBM**
- **Spherical particles covered with small particles were simulated in order to obtain a detachment criterion depending on the flow situation**

References

- **Dietzel, M. Ernst, M. and Sommerfeld, M. (keynote): Application of the Lattice-Boltzmann-Method in two-phase flow studies: From point-particles to fully resolved particles. Proceedings of ASME-JSME-KSME Joint Fluid Engineering Conference 2011 (AJK2011-FED) July 2011, Hamamatsu, Shizuoka, Japan, Paper No. AJK2011-04033.**
- **Dietzel, M. and Sommerfeld, M.: Numerical calculation of flow resistance for agglomerates with different morphology by the Lattice-Boltzmann Method. Powder Technology, Vol. 250, 122–137 (2013)**
- **Ernst, M., Dietzel, M. and Sommerfeld, M.: A lattice Boltzmann method for simulating transport and agglomeration of resolved particles. Acta Mechanica, Vol. 224, 2425-2449 (2013)**
- **Cui, Y., Schmalfuß, S., Zellnitz, S., Sommerfeld, M. and Urbanetz, N.: Towards the optimisation and adaptation of dry powder inhalers. International Journal of Pharmaceutics, Vol. 470, 120 – 132 (2014)**
- **Cui, Y. and Sommerfeld, M.: Forces on micron-sized particles randomly distributed on the surface of larger particles and possibility of detachment. International Journal Multiphase Flow, Vol. 72, 39 – 52 (2015)**